



Three decades of sea level multi-mission satellite data reprocessed to improve mesoscale quality while ensuring climate scale consistency

Cécile Kocha¹, Marine Liévin¹, Yann Pageot², Clémence Rubin³, Victor Quet¹, Franck Octau³, Marie-Isabelle Pujol¹, Pierre Prandi¹, Sabine Philipps¹, Gerald Dibarbouré⁴, Isabelino Denis⁴, Carolina Nogueira Loddo⁵, François Bignalet-Cazalet⁴

¹ Collecte Localisation Satellite, Ramonville Saint-Agne, 31520, France

² CELAD, Balma, 31130, France

³ ALTEN, Toulouse, 31300, France

¹⁰ ⁴ Centre National Etudes Spatiales, Ramonville Saint-Agne, 31520, France

⁵ EUMETSAT, Darmstadt, 64295, Germany

Correspondence to: Cecile Kocha (ckocha@groupcls.com)

¹⁵ **Short Summary.** 30 years of satellite altimetry data were reprocessed in 2024, using state-of-the-art research algorithms and models. The so-called DT-2024 sea level dataset provides a homogenous and consistent set of observations from 15 satellites and 5 climate reference altimeters. This new dataset is shown to improve mesoscale quality and consistency, particularly over coastal and polar areas, as well as the long-term stability for climate research.

²⁰ **Abstract.** Since the launch of TOPEX/Poseidon in 1992, more than 15 satellite altimetry missions have gathered measurements of ocean surface topography. These observations contributed to significant advancements in our understanding of ocean dynamics in the open ocean, coastal and polar areas and at scales ranging from 10 km and a few days to global averages over decades. Heterogeneity across missions and long update cycles of altimeter instrument processing facilities remains a challenge to assemble a multi-mission, consistently processed, state-of-the-art dataset serving the needs ²⁵ of various user types from data assimilation into ocean circulation models to climate science.

In this context, the Delayed Time DT-2024 satellite altimetry reprocessing is a massive endeavor spanning over more than a 100 years' worth of data, from 3 decades, 15 satellites, and 5 climate reference altimeters. In our effort to enhance the user-oriented "reliability" of sea level measurements, we focus on the refinement of altimetry satellite standards (radar processing ³⁰ algorithms and geophysical models) and on the cross-mission consistency. Reliability is here treated as a multi-dimensional spectrum encompassing coverage, precision, accuracy, and stability. These four pillars are essential, not only to capture



short-term ocean variability (large and small eddies) for the open, coastal and polar oceans, but also to detect seasonal and long-term climate signals such as global mean sea level rise.

35 The DT-2024 standards introduce new radar processing algorithms and geophysical corrections. In coastal areas, the error is reduced by 5,6 cm² (or 17%), enhancing monitoring of applications as storm surges and upwelling. In polar regions, error reduction of variance at crossovers exceed 7,7 cm² (or 27%) in the Arctic and 5,9 cm² (or 18%) in the Antarctic, potentially enhancing observation of freshwater fluxes and circulation around ice-covered zones. In open ocean, the error of sea surface height variance at crossovers is reduced by 1,2 cm² (or 6%). Although the contributions of each standard are relatively
40 balanced in the open ocean, the significant improvements observed in coastal and polar regions are largely attributable to the FES-22B tide model, which alone contributes approximately 70% of the gains in these areas. Additional gains come from the TUGO atmospheric correction (forced with ERA5), the CLS/DTU/SIO Hybrid-23 mean sea surface and updated instrumental corrections. These refinements could potentially aid in the detection of mesoscale features, contribute to the assimilation of data into ocean models, and offer insights into dynamic processes such as fronts and internal tides. These
45 improvements stack up with similar gains from previous reprocessing campaigns (e.g. DT-2021), highlighting a continuous progress made in satellite altimetry with every reprocessing cycle since the nineties.

Ensuring the stability of sea level measurements is also crucial for accurate climate monitoring and analysis (Cazenave et al., 2019, Meyssignac et al. 2023). To support climate applications, the DT-2024 definition was rigorous because new
50 algorithms could affect the sea level trends of the multi-mission dataset. To ensure the accuracy and consistency of sea level measurements over time, we align all coverage and precision missions on a unified reference frame based on the reference climate altimeter series. The reference altimeters are extremely consistent with one-another thanks to their so-called tandem phases (formation flight) although we compute the static offsets between subsequent reference altimeters to reduce residual offsets (and to estimate the uncertainty of the transition between reference altimeters). Comparisons with independent in-situ
55 tide gauges yield an agreement within 0.01 mm/year for the regions where tide gauges are located.

The DT-2024 Level-2P dataset is available to users for all the altimeter missions on AVISO+ (<https://doi.org/10.24400/527896/a01-2025.004>). The Level-3 and Level-4 counterparts are available on the Copernicus Marine Service catalogue (<https://marine.copernicus.eu>) and C3S (<https://cds.climate.copernicus.eu/>).

60 1 Introduction

Satellite altimetry has revolutionized our ability to monitor sea level variations since the launch of TOPEX/Poseidon in 1992. In the past thirty years, more than 15 satellite altimetry missions have been operated, collecting more than 100 years' worth of geophysical record. These missions are operated by different space agencies, and they are based on various



different instrumental configurations and orbital parameters. Their combined measurements have significantly advanced our
65 understanding of ocean dynamics and sea level change. Nevertheless, the intrinsic heterogeneity among such a constellation may create persistent challenges in constructing a long-term, homogeneous, and stable view of the ocean surface topography for operational, research and climate applications.

Each altimetry mission plays a specific role in the monitoring of ocean surface topography. The so-called “reference”
70 altimeters are TOPEX/Poseidon (TP), Jason-1/2/3 (J1, J2, J3), and Sentinel-6 Michael Freilich (S6A): they form the backbone of the climate-quality records thanks to their extreme stability, specific orbit properties, extremely precise tandem phases (formation flight during the commissioning phase), and unbroken record of 3 decades.

Moreover, other altimetry satellites, such as ERS-1/2 (E1, E2), ENVISAT (EN), CRYOSAT-2 (C2), SARAL/AltiKa (AL)
75 and Sentinel-3A/3B (S3A, S3B), provide denser coverage of higher latitudes, while GEOSAT Follow-On (GFO), HaiYang-2A/B (HY-2A, HY-2B), and SWOT improve spatial and temporal resolution through complementary orbits. Some of these altimeters are technology demonstrators (e.g. SARAL with Ka-band, Cryosat-2 with Doppler altimetry and interferometry) while others are operational carbon copies of their predecessors (e.g. S3B, JA2 and JA3) ensuring consistent designs
80 throughout one or two decades. Moreover, Climate-oriented missions prioritize long-term stability and accuracy, with precision considered a secondary benefit. Conversely, missions such as Sentinel-3 are primarily designed for high precision and spatial/temporal coverage, whereas stability is desirable but not required for the mission’s success.

The sea surface height anomaly¹ (SSHA) retrieved from satellite altimetry technology is determined by measuring the distance from the satellite to the target surface, using the round-trip time of a radar pulse. Despite numerous corrections to
85 account for instrumental and environmental effects, residual biases may remain in the measurements, often exhibiting spatial and temporal correlations (Escudier, et al. 2017). To that extent, it is important to select the best geophysical models and environmental corrections for each mission, and to perform a consistent cross-mission homogenization so that various satellites can be compared, combined or assimilated easily.

90 Over the past 30 years, altimetry processing standards have evolved, largely driven by mission-specific instrumentation and the frequency of data reprocessing. However, some Level-2 products have not been regularly updated, limiting homogenization efforts. To maintain data quality at the highest level and ensure maximum homogeneity across all missions,

¹ Some authors also use the term sea level anomaly (or SLA). Both terms and acronyms are equivalent. They are defined as the difference between the sea surface height measured by the altimeter, corrected from series of instrumental and geophysical models, and a temporal average over a very long period (the mean sea surface height, also known as mean sea surface model or MSS).



a full reprocessing of the datasets is performed approximately every 3 to 5 years: DT2018 (Taburet et al., 2019), DT2021 (Lievin et al., 2020). The so-called Data Unification and Combination System (DUACS) was designed to manage this
95 complexity: it handles the homogenization, cross-calibration and blending altimetric datasets since the late 1990s (Dibarbour et al., 2021). It is operated in near-real-time and delayed-time to generate Level-2P, Level 3 & Level 4 products which are disseminated by the Copernicus Marine Environment Monitoring Service and the Copernicus Climate Service. DUACS produces consistent, continuous time series that are used by a large number of research teams to study the ocean circulation and mesoscale turbulence, as well as global and regional mean sea level trends.

100

A central question guiding our efforts is: *How can we improve the mesoscale observability and inter-mission consistency of satellite altimetry to construct a reliable sea level record at climate scales?* In this context, the latest iteration of the Delayed Time (DT) Level-2P/3 dataset was produced in 2024 with a massive reprocessing of 30 years from 15 satellites. This paper
105 presents the key advancements achieved, including refined geophysical corrections and improved instrument processing algorithms. Furthermore, we detail the methodology used for alignment between reference missions. We also emphasize the pivotal role of the Copernicus Sentinel-6 MF/Jason-CS mission, which now serves as the new regional reference: it ensures the continuity and stability of the sea level record as we enter the fourth decade of satellite altimetry.

The paper is organized as follows. Sect. 2 provides an overview of the Level-2 input products, along with the Level-2P
110 standards and models that define DT-2024. Sect. 3 presents the resulting improvements across various oceanography usages. Sect. 4 then focuses on the alignment of the reference altimeters that provide a seamless climate record. Sect. 5 compares SLA from altimetry with independent in-situ tide gauge measurements. Finally, Sect. 6 discusses the past and future evolutions of these Level-2P/3 products.

2 Altimetry standards impact on sea level consistency

115 2.1 Methodology to select new DT24 standards

To improve mesoscale observability, coastal accuracy, or polar performances, a long list of candidate algorithms were tested
120 (at least 2 or 3 for each altimeter correction and model). To select the best option, we use a somewhat classical metric used in altimetry Calibration/Validation studies (e.g. Cadier et al., 2024): the reduction of variance at crossover points. When two altimeter tracks cross over, they provide two independent measurements for the same location (with a time lag of a few hours or a few days). The difference in the two SSH measurements on the crossover point is the sum of the natural ocean variability (e.g. displacement of ocean eddies) and altimetry measurement errors (biases and noise). Assuming that altimeter



errors are independent from the signal of interest ², changes in the SSHA difference at crossover points is a partial measurement of the altimeter errors. The crossover points are binned in space or in time. When a new algorithm candidate is tested, we analyze the change in crossover variance, which is a good indicator of the gain or loss in altimeter errors (and 125 where/when the gain is maximal).

For a single mission, crossover points evaluate the coherence between ascending and descending ground tracks, or the temporal variability of the errors. In a multi-mission context, they measure the agreement between intersecting tracks from different satellites. We compute the variance at crossover points within 10 days to minimize the impact of residual 130 systematic errors and to compare different satellite altimeter data (Jettou et al., 2023; Stammer and Cazenave, 2018). Assuming equal and independent errors, the crossover variance is halved to yield the total error of individual satellite measurements.

Furthermore, in addition to the crossover metric, we analyze the variance of the SSHA as a function of various criteria (e.g. 135 distance to shore, or latitude, or significant wave height) to verify that each variance reduction is found where it was predicted by the reference paper of a given correction. To illustrate, new geoid models will result in a SSHA variance reduction that is geographically distributed along geodetic features such as mid-ocean rifts and sea-mounts, while improvements of the wet troposphere correction will reduce the variance in very different regions.

140 We also evaluate the impact of tentative changes on regional and global sea level trends, with a focus on reference missions. When we detect significant discrepancies or drifts, we trace back their source to assess the overall consistency using independent, stable observing systems. Lastly, we also rule out the existence of significant regional biases, trends or random errors: if a new correction or algorithm introduces a difference, it has to be justified and consistent with literature.

145 All these analyses produce a massive amount of metrics for each tentative change. For the sake of clarity and concision, this paper reports only a few notable examples for the new DT-2024 standard, but it does not present the validation of each item, let alone discuss the (many) alternative corrections that were studied but not selected.

2.2 Overview of the DT-2024 standards

The DT-2024 standard introduces a large number of updates with respect to the previous iteration DT-2021 (Fig. B 1), as 150 shown by the number of green boxes in Fig. 1. Each item is publicly available, and has been published, with a clear demonstration of their individual contributions for at least one altimetry satellite and usage. To assemble DT-2024, we

² This is not always strictly true for some error sources, but beyond the scope of this paper.



examine their strengths and weaknesses in an integrated context and with the aim to perform a multi-mission and multi-usage harmonization.

155 Updates in DT-2024 are also color-coded (e.g. blue and orange chevrons) by their primary area of impact: mesoscale features, long-term stability, coastal accuracy, or polar performance. The description of the major contributors and the reasons for these improvements are detailed below: Sect. 2.3 describes the changes in the altimeter radar processing, Sect. 2.4 covers the geophysical and environmental corrections and Sect. 2.5 tackles the mean sea surface reference.

MISSION	Poseidon	Topex	Jason 1	Jason 2	Jason 3	ERS-1	ERS-2	ENVISAT	Geosat FO	SARAL	Cryosat 2	HY 2A	HY 2B	Sentinel 3A	Sentinel 3B	Sentinel6A/JasonCS	SWOT nadir
L2 version	GDRF [20]		GDRE	GDRD	GDRF	OPR		RA2/MWR V3.0	1st version	GDRF	BC/BD (>c259)	Unknown		BC005		F08/F09 (>c122) /G01(>c160)	GDRF
RETRACKING	MLE3 Numerical LRM	LRM	MLE4	MLE4 LRM	MLE4 LRM	LRM		MLE3 (OCE-1) LRM	Onboard tracker LRM	MLE4 LRM	SAMOSA 2.3 SAR/LRM		MLE4 LRM		SAMOSA SAR	Numerical (SAR SAMOSA <c120)	MLE4 LRM
ORBIT	GSFC std 18	POE-F		POE-F		Reaper		POE-F	GSFC	POE-F	POE-F	POE-D	POE-F		POE-F	POE-F	POE-F
IONOSPHERIC CORRECTION	DORIS	Filtered dual frequency	Filtered dual frequency [5] (SSB C band)		Filtered dual frequency [8]	NIC09 [9]	GIM [6]	Filtering [19] & GIM (>c65)			GIM [6]				Filtered dual frequency	Filtered dual-frequency LRM	Filtered dual frequency
SEA STATE BIAS	2D TP		2D J1 Non parametric [13]	2D J2 Non Parametric [11]	2D J3 MLE4 Non parametric [16]	BM3 [4]	Non parametric [7]	2D EN Non parametric [14]	Non parametric [10]	Non parametric [12]	Non parametric BC [15]	Non parametric [11]	L2 product	Non parametric [17]	2D J3 MLE4 Non parametric [16]	2D J3 MLE4 Non parametric [16]	
WET TROPOSPHERE	TMR radiometer	JMR radiometer	AMR radiometer	AMR radiometer		GPD+ [3]	MWR radiometer	Radiometer & HRES model	Neuronal Network V4	GPD+ [3]	HRES model	HRES model & radiometer (>c42)		GPD+ [25]	AMR radiometer	HRES model	
DRY TROPOSPHERE								ERA5 (1-hour) model based									
DYNAMICAL ATMOSPHERIC																	
OCEAN TIDE																	
INTERNAL TIDE																	
POLE TIDE																	
SOLID TIDE																	
MEAN SEA SURFACE																	

Legend: Meso-scale (blue), Stability (orange), Coast (purple), Polar (green), STD 24 (yellow), STD 21 (light green), STD 18 (light blue), STD 14 (light orange), STD 10 (light purple).

160 **Figure 1 Sea level standards table for DT-2024.** The shades of gray (from light to dark) and green indicate when each standard changed since DT-2010. Other colors highlight mesoscale improvements, stability improvements, coastal improvements and polar improvements. Sources: [1] (Cartwright D. E. and Taylor R. J. 1971) ; (Cartwright D. E. and Edden A. C. 1973) [2] (Desai S. 2015) [3] (Fernandes M J. 2016) [4] (Gaspar 1994) [5] (Guibbaud 2015) [6] (Ijima 1999) [7] (Mertz 2005) [8] (Nencioni 2022) [9] (Scharroo 2010) [10] (N. L. Tran 2010) [11] (N. P.-C. Tran 2012) [12] (N. , Tran 2019) [13] (N. Tran, SSB Activity 2015) [14] (Tran N. 2017) [15] (N. Tran, "ESL Cryosat-2: Tuning activities(wind speed and SSB)" 2018) [16] (Bignalet-Cazalet 2021)[17] (N. Tran 2021) [18] (Zaron 2019), [20] (Forster 2025) [21] (L. Carrere 2022) & (F. H. Lyard 2024), [22] (Laloue 2025) [25] (Fernandes 2024)

2.3 Altimeter input dataset reprocessing

170 Space agencies and the altimetry community are continuously enhancing data processing techniques to improve the precision and accuracy of altimeter measurements. Regular data reprocessing of level 2 datasets enables the integration of the state-of-art waveform retracking algorithms, thereby enhancing the quality and consistency of altimeter products. While agencies occasionally coordinate to adopt the same standards (e.g., GDR baseline F or G), these updates are not implemented simultaneously, let alone uniformly across all past and present missions.

175 In this context, the contribution of the newly developed ocean numerical retracker (Buchhaupt 2019; Dinardo et al., 2023, Salvatore et al. 2024), implemented into the S6A operational processing chain, is noteworthy as it offers improved stability in global mean sea level measurements compared to the historical MLE-4 retracker. This major improvement is achieved by



incorporating the in-flight radar Point Target Response into the waveform fitting model, which compensates for potential altimeter drifts and thus mitigates instrumental ageing issues (Dinardo et al, 2023; Cadier et al, 2024). This retracking
180 solution also avoids the need to use correction tables to compensate for the Gaussian approximation of the PTR in the waveform model, thereby preventing potential errors associated with the computation of these corrections (Cadier et al, 2024). In this regard, the numerical retracker significantly reduces sea-state related effects, leading to a 60% reduction in the sea surface height anomaly bias correlated to significant wave height, between the Sentinel-6 MF low resolution numerical retracker and Jason-3 MLE4 retracker (Cadier et al, 2025). These results further enhance the already excellent continuity
185 between the two missions, improving the stability of global mean sea level estimates by mitigating instrumental drifts and sea-state-related biases, as discussed in Sect. 4.2.

On Jason-3 mission, two recently reprocessed retrackings are available for GDR version F: one is based on the historical MLE4 approach and the Adaptive retracker (Thibaut et al, 2021), which inherits the processing methodology initially
190 developed for the CFOSAT mission (Thibaut et al, 2021; Tourain et al, 2021). To maintain mean sea level (MSL) continuity and to ensure consistency within the time series, the MLE4 retracker was chosen for DT-2024, due to its close similarities with the S6A low resolution numerical retracker, particularly in their response patterns to varying sea state conditions. Prior to integration into our selection, we had to correct the MLE4 range jumps observed after the instrument reset (cycles 57 to 85) by aligning with the adaptive retracker—less sensitive to such changes—to ensure global mean sea level continuity.

195 TOPEX benefits from a recent Level-2 reprocessing by NASA and CNES using MLE4 and MLE3 retracker solutions for Ku and C band respectively. The new TOPEX/Poseidon dataset exhibits global, regional, and coastal improvements in accuracy and precision. The reprocessing also leverages improvements from the NASA's Goddard Space Flight Center precise orbit determination, an enhanced microwave radiometer calibration, and a new 2D sea state bias model from the University of
200 Colorado Boulder (Foster et al, 2025). In the previous version of TOPEX side A, a drift was observed, confirmed with 3 independent methods, and corrected empirically (Ablain et al, 2017). For this new reprocessing, studies are underway to determine if the reprocessed dataset TOPEX-A still requires correction.

Sentinel-3A and B also exhibit improvements in accuracy and measurement stability due to the Level-2 reprocessing in
205 baseline collection 5 from EUMETSAT. It includes updates to the 1 Hz generation method with strict MQE screening, enhancements from the application of the range walk correction (Scagliola et al, 2021; Dinardo et al, 2023) and CoG CAL1 for long-term stability, and exact zero masking (Lucas, 2023). The USO reading correction was already included in the DT-2021 Sentinel-3B 3.1 version using early implementations of this correction (EUMETSAT, 2021).

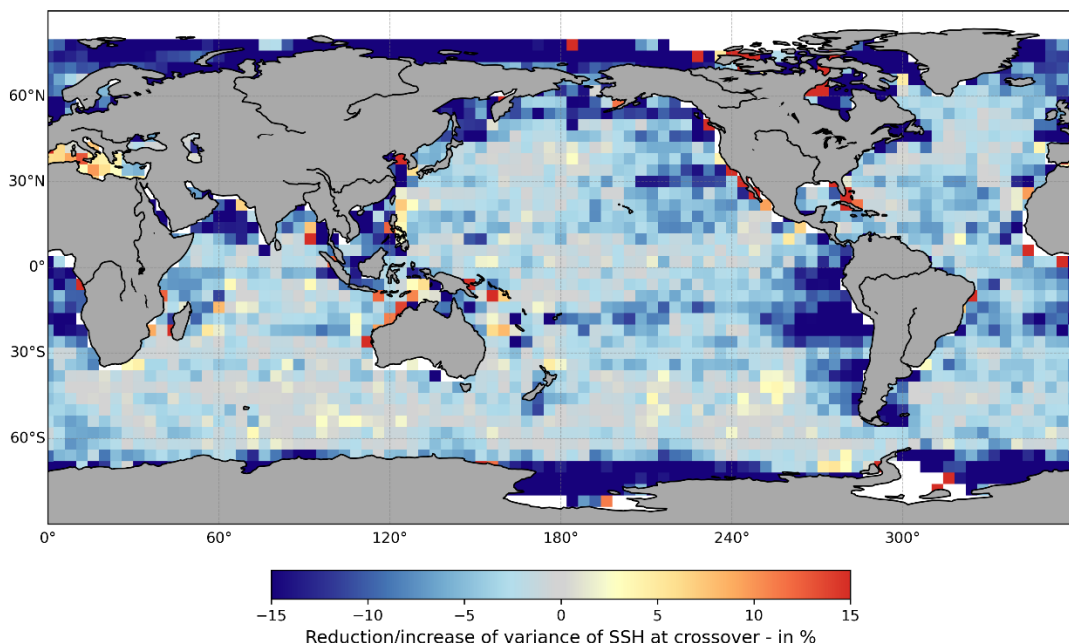


2.4 Geophysical and environmental corrections

210 The raw altimeter sea surface height anomaly is corrected from a set of geophysical corrections and models: the altimeter range is indeed affected by various path delay sources from the atmosphere, and the radar echo can be distorted by the ocean surface waves. Lastly, various high-frequency ocean signals must be dealiased from the altimeter data (e.g. the barotropic response to tides or atmospheric forcing). Escudier et al. (2017) explain how the so-called geophysical and environmental corrections and models intend to mitigate all these effects. But none of them are perfect, and their residual errors are very
215 significant contributors to the final error budget of the altimeter data. To that extent, each of these models was revisited in the DT-2024 standards to improve the final quality of the dataset. For the sake of concision, this paper discusses only 3 major changes in DT-2024, although more than 10 were studied and upgraded (Fig. 1).

2.4.1 Ocean tide correction

For DT-2024 products, various state-of-the-art ocean tides models were evaluated and the FES22 model was selected,
220 replacing the FES14B model used in the previous release DT-2021 (Carrere et al, 2016). Detailed by Carrere et al. (2022) and Lyard et al. (2024), the FES22 model offers a spatial resolution improved by a factor of 8, and it benefits from increased in situ data assimilation and improved regional bathymetry, especially in coastal and polar regions.



225 **Figure 2 Difference between the variance at crossover points for the sea surface height using FES22 version versus FES14B.**
Computed with SARAL/AltiKa cycles 1-169. Expressed in % of SSHA variance. Negative values indicate a reduction of the SSHA crossover variance with FES22.



The difference between the variance of the SSHA at crossovers using FES22, and the counterpart FES14B is shown in Fig. 2. A decrease in variance indicates better signal consistency, i.e. a reduction in bias or noise errors from tides residuals³. The 230 error at crossovers is reduced everywhere in the global ocean. It can be up to 15% more in polar regions, coastal areas, and the continental shelf.

Furthermore, ocean tide impacts the global trends by less than 0.06 mm/year for TOPEX, Jason-1 to Jason-3 reference 235 missions. By design of the correction, ocean tides should barely impact long-term trends. Yet, Ray and Schindelegger (2025) describe that if the leakage from ocean mesoscale (or altimeter errors) changes over time, it will impact ocean-tide trend estimation. In this context the long time series of reference Climate altimeters might be instrumental to explore, quantify and mitigate such a potential leakage of ocean variability and altimeter errors in tides models.

2.4.2 Dynamical atmospheric and dry tropospheric corrections

The ERA5 meteorological model was used in the DT-2021 reprocessing for the dynamical atmospheric correction (DAC) 240 and the dry tropospheric correction. Based on the 2016 HRES operational model version (ECMWF 2024), the ERA5 reanalysis (Herbach et al, 2023) was shown to be seamless and continuous for the climate time series, as opposed to the regional and global jumps created by operational ECMWF model upgrades. Moreover, ERA5 provides a higher temporal resolution than the operational counterpart (1h vs 6h), which allows a more realistic modeling of high-frequency events for atmospheric corrections.

245

Using the dry tropospheric correction and the dynamic atmospheric correction based on ERA5, instead of the HRES operational model, removes a sea level anomaly regional trends up to 0.25 mm/year, and regional trends up to 1 mm/year: these 250 artificial trends actually originated in various offsets caused by updates of the operational ECMWF model. Moreover, with a more recent model version, the atmospheric reanalysis significantly improved the quality of the atmospheric corrections for older missions. A new DAC-ERA5 has been produced using the TUGO ocean model forced by the ERA5 fields. TUGO is a barotropic ocean model which leverages the finer mesh and better bathymetry inherited from the FES14B developments (Lyard et al, 2021). It also features better interpolation of wind and pressure variables, and optimized internal wave drag dissipation (Carrere, 2023). The TUGO model replaced its predecessor (MOG2D) for operational use in 2023. TUGO was shown by Carrere et al. (2023) to improve mesoscale accuracy, especially along coasts, in polar regions, and 255 over the continental shelf.

³ Because the tide model assimilates altimeter data, a reduction of the SSHA variance could also be interpreted as oceanic variability leakage in the tides models. However here, the regions exhibiting a variance reduction are clearly related to bathymetry and mesh resolutions, large tides signals, known deficiencies of FES14, rather than other oceanic variability (e.g. western boundary currents are not clearly visible in Fig. 2).



As a result, the new DAC-ERA5 correction reduces the sea surface height variance between 1993 and 2021 by up to 1 cm^2 for the global ocean. Furthermore, for the coastal ocean (less than 10 km from the coast), the SSHA variance reduction is much larger: 2.5 cm^2 for the TOPEX, and 1.5 cm^2 for Jason-1 (Lievin et al, 2020). For recent missions, the ERA5 reanalysis 260 yields a performance of the same order as the HRES operational counterpart: despite its coarser spatial resolution, ERA5 has a higher temporal resolution. Lastly, for the dry tropospheric correction, the use of ERA5 reduces the sea surface height variance at crossover by 0.16 cm^2 for the global ocean, and by 0.6 cm^2 in low-pressure areas.

In other words, ERA5 does not significantly improve mesoscale variability for recent missions, because HRES is already 265 excellent since the early 2020s. However, ERA5 provides better climate-focused stability, and it does improve the quality of older satellites. The DT-2024 reprocessing ensures a seamless continuity of the DAC and the dry tropospheric correction over the entire period (Kocha et al, 2023).

2.4.3 Wet tropospheric correction

The altimeter path delay is affected by the wet troposphere. It is generally corrected by an onboard microwave radiometer. 270 Some altimetry missions were designed without a radiometer⁴, and some ageing missions have lost theirs⁵, and the alternative is then to use a wet troposphere correction (WTC) derived from an atmospheric model. The radiometer-based correction remains the most precise WTC alternative because measurements are co-located with the altimeter, ensuring space/time consistency, as opposed to the interpolated/smoothed model correction. The radiometer WTC is better by approximately 1 cm^2 for the global ocean and much more in active troposphere regions.

275

Because the microwave radiometers are highly sensitive to in-flight conditions (e.g. thermal control, or safe-hold mode events), a rigorous calibration procedure is usually applied in the Level-2 product, in order to get a correction as seamless and stable as possible. For the reference climate altimeters (TOPEX, Jason series and Sentinel-6 MF), this calibration is 280 performed by the Jet Propulsion Laboratory (JPL). A key innovation of recent climate altimetry missions is the use of cold-sky maneuvers, where the satellite is rotated to observe the cosmic microwave background, providing a stable external reference through the same optical path as Earth scenes. These maneuvers, combined with on-Earth targets, provide a two-point calibration that is essential for long-term stability (Brown and Islam, 2017). Given the radiometer's dominant contribution to the mean sea level error budget (Guerou et al., 2023), the radiometer WTC is often scrutinized and compared with atmospheric model reanalysis.

⁴ E.g. CRYOSAT-2 was designed to study the cryosphere in polar regions where the wet troposphere is not critical

⁵ E.g. the microwave radiometer of Geosat Follow-On (GFO) had to be switched off to alleviate power constraints on the satellite, after 8 years of excellent operations



285

The quality of radiometer data can be affected by land or rain contamination, so the GPD+ correction from Fernandez et al. (2024) combines radiometer data, Special Sensor Microwave Imager (SSMI), and model data to improve accuracy when radiometer measurements are deemed unreliable, such as near coasts and sea-ice. Figure 3 shows that the variance of sea 290 surface height at crossover points is significantly reduced at coasts and over rainy areas for Sentinel-3A. Variance of SLA is reduced by up to 5 cm² at 10 km of the coast for Sentinel-3A.

While combining different sources can modify global or regional trends, this is not the case for Sentinel-3 GPD+ correction. The impact on the regional MSL trend is less than 0.4 mm/year in polar regions (the most impacted areas) and less than 0.02 mm/year over the entire Sentinel-3A period. Thus, the mesoscale quality is improved without any significant side-effects on 295 the climate series trends.

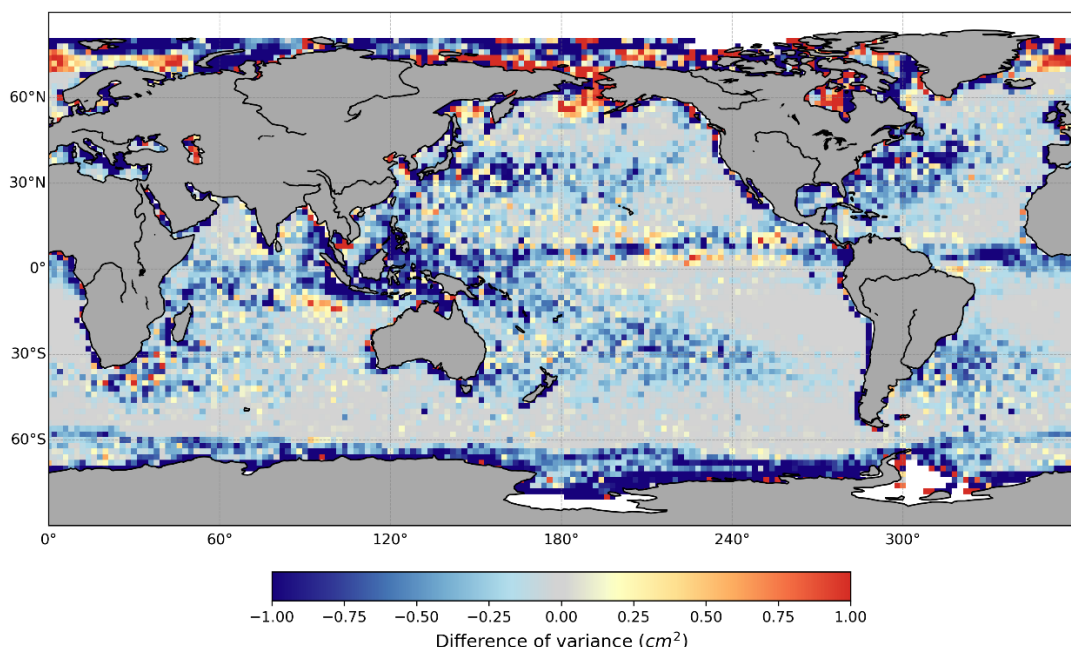


Figure 3 Variance at crossover points of sea surface height using wet tropospheric correction from GPD+ versus radiometer on Sentinel-3A (cycles 3-70). Negative values mean reduction of the variance with GPD+ version.

2.5 Mean sea surface

300 The sea surface height measured by the altimeter is dominated by the geoid, i.e. the topography signatures of the earth gravity field, and this effect is removed by removing the mean sea surface (MSS) modelled using 30+ years of data from various missions and orbits. While the larger scales of the geoid are relatively well known since the end of the 90s, the scales smaller than 30 km (e.g. signature on the SSH of sea mounts or mid-ocean rifts) is still an active research topic. In this



context, we have evaluated the latest iterations of the MSS models from various groups (e.g. DTU, Scripps, CNES) to
305 quantify their strengths and weaknesses.

The best candidate for DT-2024 was found to be the Hybrid 2023 (H23) model that combines three recent MSS models to
leverage their specific advantages (Laloue et al, 2025). Indeed, the CNES/CLS 2022 (Schaeffer et al, 2023) model better
resolves large and medium structures with an optimum consideration of the oceanic variability. This model is mainly used in
310 coastal areas and in high variability areas. The SCRIPPS 2022 (Sandwell 2024) bring refinement of the signal at small
mesoscales in main part of the open ocean. Finally, the DTU21 model (Andersen et al, 2023) completes the coverage in
polar regions. Additionally, the Hybrid 2023 MSS model benefits from the use of high-resolution measurement (40 Hz to 5
Hz as described in Schaffer et al, 2023; Sandwell, 2024 and Andersen et al, 2023) and globally resolves smaller geodetic
structures than the previous generations (Laloue et al, 2025).

315

The improvements brought by the new MSS model was estimated in terms of reduction of variance of the sea level anomaly
(Fig. 4). In this figure, we use Sentinel-3A as this satellite is not used in the computation of the MSS H23. The importance of
having independent test data is developed by Pujol et al. (2021): it allows us to interpret the reduction of variance as a
320 reduction of the MSS errors. Figure 4 shows the reduction of the variance of the SLA (expressed in % of the SLA variance)
along Sentinel-3A tracks, when using the MSS H23 rather than H21. The variance is reduced almost everywhere, sometimes
massively: the SSHA variance reduction reaches 10 cm² in coastal regions and 2 cm² on the entire Arctic ocean (Koch et al,
2023). Similar results were obtained with HaiYang-2B although it has different ground tracks and coverage.

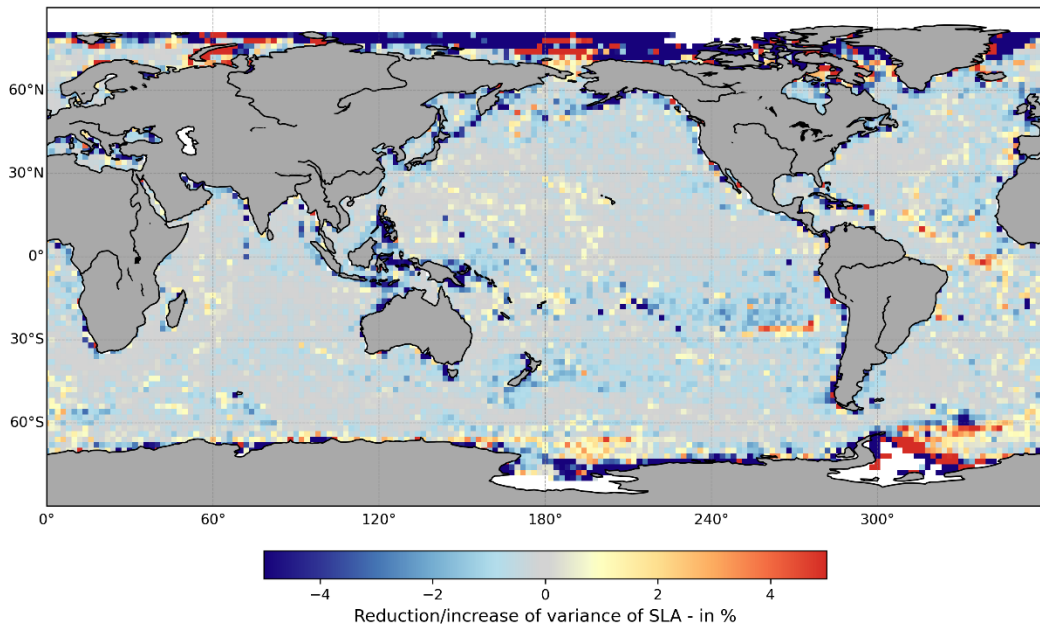
Nevertheless, some regions exhibit a large increase in SSHA variance when using the H23 MSS model. Some of them are
325 located in seasonally sea-ice covered areas where the availability of altimeter measurements is reduced. This suggests that
the MSS error is higher in these areas (as per Laloue et al, 2025). In particular, there are yellow/orange pixels aligned with
mid-ocean rifts: this behavior is caused an inconsistency between the resolution of both datasets: these structures actually
resolved by MSS H23, because the model is based on high-resolution observations (40 to 5 Hz), whereas they are too small
to be entirely resolved by the 1 Hz measurements using this metric and DT-2024 (e.g. Charayron, 2025).

330

This finding is important because future MSS models will be based on the very small and precise pixels of the SWOT
satellite (i.e. able to resolve even smaller geoid features than H23). But in the 20 to 1 Hz compression process, nadir
altimeter processing will smooth out actual geodetic features in the SSH, geodetic features that are properly resolved in the
MSS model. The discrepancy between the limited 1 Hz resolution and the very high resolution MSS model will result in a
335 SSHA variance degradation, rather than an improvement from the more precise MSS model. In other words, future MSS
models might become so precise that they may require altimetry processors to either leverage it at the full 20 / 40 Hz rate of



nadir data or require an additional layer of 1 Hz correction to be more consistent with the MSS (e.g. to account for the MSS curvature in the 1 Hz averaging window).



340 **Figure 4 SLA variance differences in % using Mean Sea Surface H23 compared to Mean Sea Surface H21 for Sentinel-3A cycles 4-89.** Negative values mean reduction of the variance with Mean Sea Surface H23 version.

3 Benefits from DT-2024 upgrades for ocean mesoscale

In the previous section, we have presented a few examples of the individual improvements from altimetry processing or geophysical corrections. But they were considered individually in a vacuum. In this section, we use a similar approach, but 345 for the entire assembled standard from Fig. 1. The rationale is to make sure that individual improvements properly sum up into a net improvement on the final product. In other words, we verify that there is no substantial correlation between the new algorithms and models ⁶.

We specifically focus on the end-to-end benefits for ocean mesoscale (global ocean, polar and coastal regions), spatial and 350 temporal consistency, and long-term sea level trend stability: any change in the MSL trend must be explained and justified from the literature.

⁶ The reason this verification is important is because many items discussed in the previous section are obtained by ingesting altimeter data (e.g. tides model assimilation or assembled into a mss model), or because they measure independently a geophysical content that is actually correlated with the true SSH (e.g. wet troposphere and air/sea interactions, sea-state bias and wave/current interactions). For both reasons, we need to rule out that a gain in one correction does not cancel out an improvement from another model.



3.1 Improvement breakdown

The Sentinel-3 crossover error reduction in Fig. 5 gives some insights on the relative importance of some components of the DT-2024 standards in various conditions: the left plot is for the open ocean, the center plot is for the coastal ocean, and the right plot is for the polar regions. To illustrate, in coastal and polar regions more than 70% of the dynamical improvements in DT-2024 stems from the new FES22 ocean tide correction. However, the open ocean exhibits a more balanced distribution of contributions across all corrections. Conversely, the improvements from new WTC algorithms are generally significant for the open ocean, whereas they are negligible for the polar ocean.

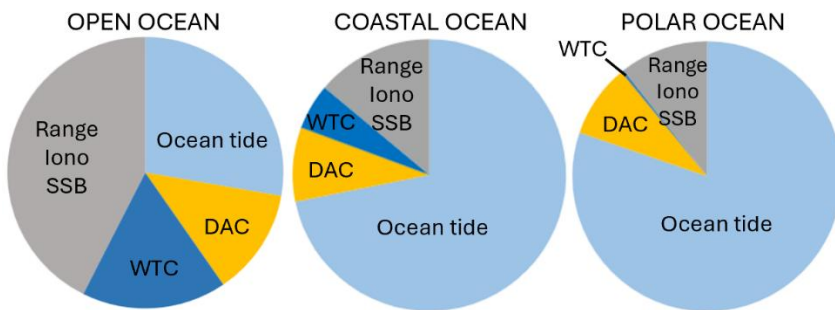


Figure 5 Fraction of the sea surface height error reduction at crossover points (improvement from DT-2021 to DT-2024 for Sentinel-3A) : Dynamic Atmospheric Correction (DAC), Wet Tropospheric Correction (WTC), Sea State Bias (SSB), ionospheric correction (IONO). From left to right: open ocean (bathymetry deeper than 1000m, latitude below 50°N/S), coastal ocean (less than 100km from the shoreline) and at polar ocean (latitudes higher than 66°N/S).

360

While these plots are arguably expected from the reference papers of individual corrections, this result is a reminder that the DT-2024 has to balance a wide range of improvements with different goals: some algorithms and models were selected to provide a better precision, to resolve smaller eddies in the open ocean, while others provide little to no benefit for this usages because they are focused on coastal and sea-ice robustness. Like all altimetry standards, these items are gauged according to 370 different criteria, the final standard is a trade-off between them.

Note that, although crossover error reduction is the most consistent diagnostic for assessing data coherence, it only gives insights on the temporal variability of the errors. Conversely, time-invariant components such as the mean sea surface, or slowly evolving biases (e.g. long period of tides and WTC), are not visible in the metric from Fig. 5, even though they play a 375 major role in SLA variance reduction. To illustrate, the MSS model alone accounts for 10% of the overall SSHA gain in some regions (Laloue et al, 2025), but the two measurements of a crossover are by definition located in the same location: the MSS cancels out in a crossover difference, and the better geoid is not captured by a crossover metric.



3.2 Temporal evolution

In this section, we gauge the evolution of the gain from the DT-2024 standards over the 30 years of altimetry (Fig. 6). In 380 particular, we want to assess if certain corrections have a more impact during specific periods. This analysis helps identify potential shifts in data quality throughout the altimetry record.

Over the entire reprocessing period, and the global ocean, the median gain at crossover variance for all missions is 2.4 cm^2 (1,1 cm rms). This indicates an improvement in data accuracy and consistency of 6% for the global ocean. The annual 385 oscillations originate in the seasonal cycle of sea-ice coverage, because the SSHA variance reduction is larger in the Arctic than for the global ocean.

The DT-2024 reprocessing exhibits higher gains before 2002, primarily from the TOPEX reprocessing. After 2016, the new 390 DAC TUGO model is used with the ERA5 model, resulting in notable improvements over the DT-2021 counterpart based on MOG2D forced by operational ECMWF 6h fields.

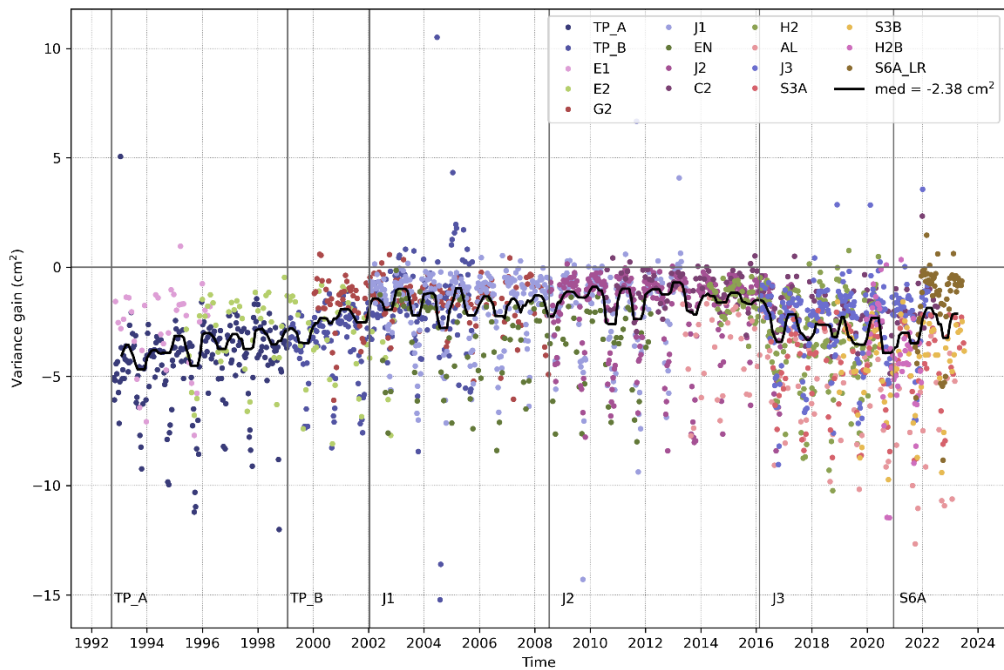
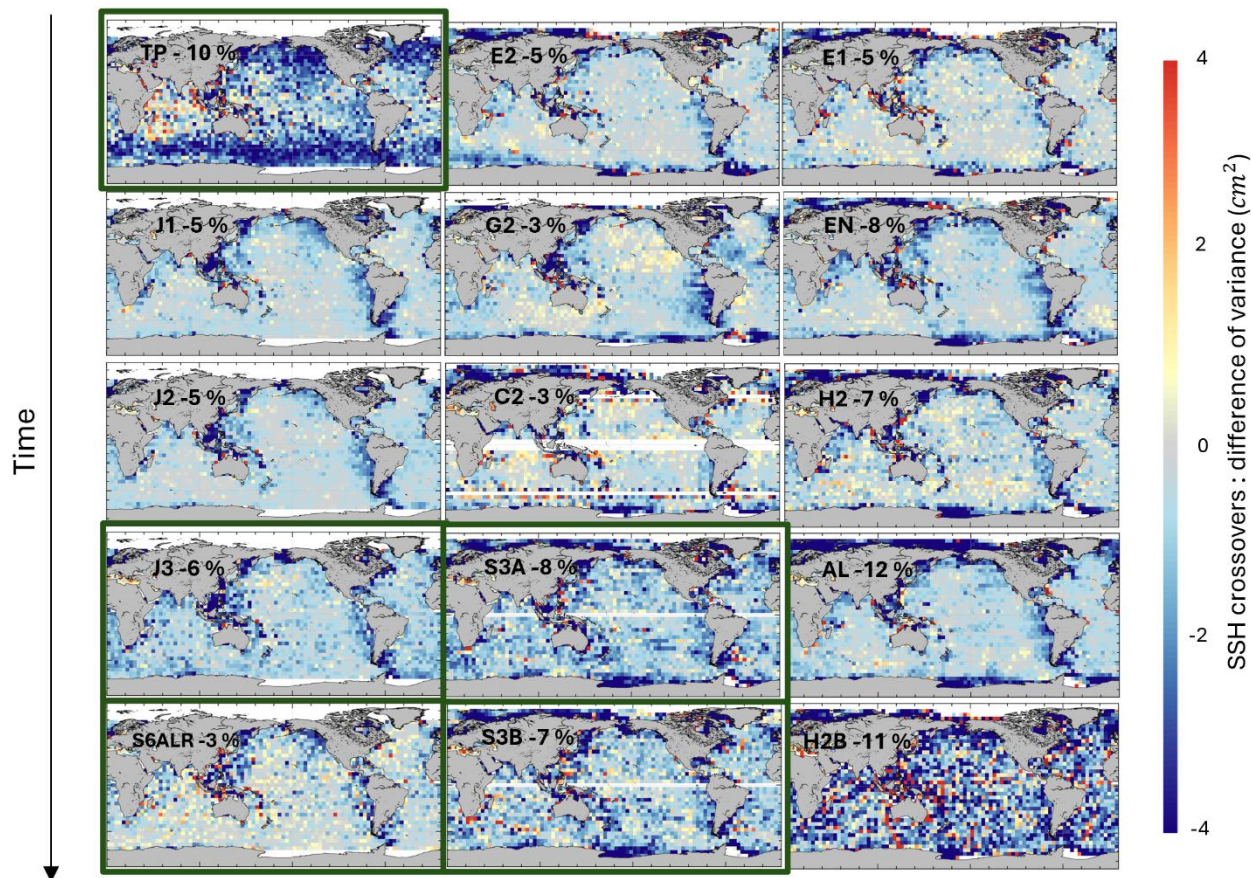


Figure 6 Difference of variance at sea surface height crossovers for each mission between reprocessing DT-2024 - DT-2021. An 8-month rolling median has been added in black.



395 3.3 Geographical distribution

The geographical distribution of the improvements from DT-2024 is illustrated in Fig. 7. For all altimeters, we observe a higher reduction in variance at crossovers located in coastal areas and high latitudes (shown in dark blue), principally thanks to new geophysical corrections such as FES22 and DAC TUGO. Missions reprocessed at level 2 (highlighted in green) generally show more significant gains in SSH crossover variance, with different regional patterns indicating the importance 400 of radar processing upgrades. For example, Topex, which benefiting of a recent level 2 reprocessing described in Sect. 2.3, shows more than a 10% reduction in SSH crossover error (Fig. 7) and the bulk of this gain actually originates in the new waveform retracker (not shown).



405 **Figure 7 Sea surface height crossover variance between standards DT-2024 minus standards DT-2021. Reprocessed Level-2 inputs
are highlighted in green.**

3.4 Coastal improvements

Coastal regions are challenging for satellite altimetry due to complex local dynamics and degraded measurement quality near the shoreline. This degradation is caused by several factors such as land contamination within the altimeter or radiometer

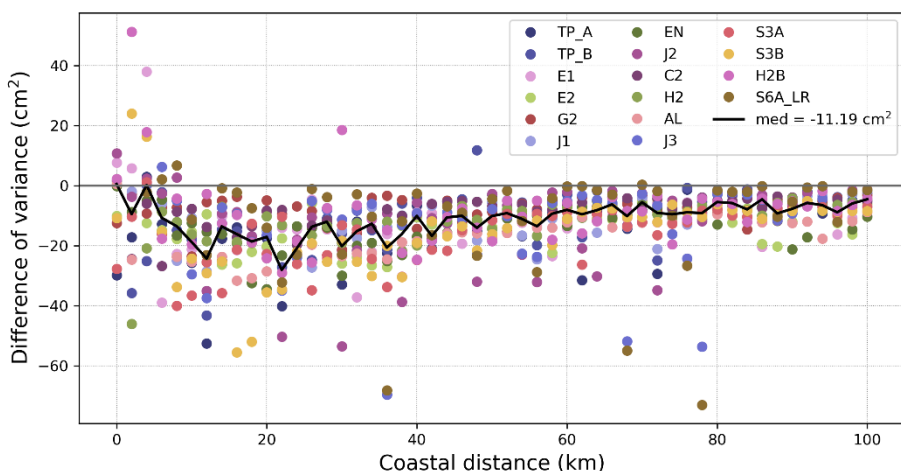


footprints, incorrect waveform retracking models, sparse altimetry coverage and imprecise bathymetry affecting the
410 precision of tides and MSS models, rapid changes in the wave spectrum and sea-state bias due to wave/current interactions...

The implementation of DT-2024 standards, particularly the inclusion of the FES22 ocean tide model, has led to notable
improvements in the estimation of sea surface height anomalies (SSHA) in coastal areas. Figure 8 illustrates a median
415 reduction of 11 cm^2 in SSH variance (i.e. 5.6 cm^2 in error reduction, 17%) is observed within 100 km of the coast across all
missions, with reductions up to 16 cm^2 for SARAL-AltiKa and Sentinel-3A. These improvements are most pronounced
between 10 and 30 km from the coast. However, within the innermost 5 to 10 km, altimetric measurements remain
significantly degraded. Land contamination affects the radar footprint, and without a coastal-optimized retracking algorithm
(not yet available in DT-2024), range errors dominate. As a result, range-derived products such as MSS models or tides will
likely exhibit limited improvement in this very nearshore zone.

420

These results confirm the benefits of the new standards to reduce some error sources in coastal regions. But it also highlights
the need for further R&D in Level-1/2 product algorithms, particularly in retracking techniques tailored to the coastal
environment, WTC and SSB upgrades, as well as geophysical models that leverage the massive coastal coverage of SWOT's
swath altimeter.



425

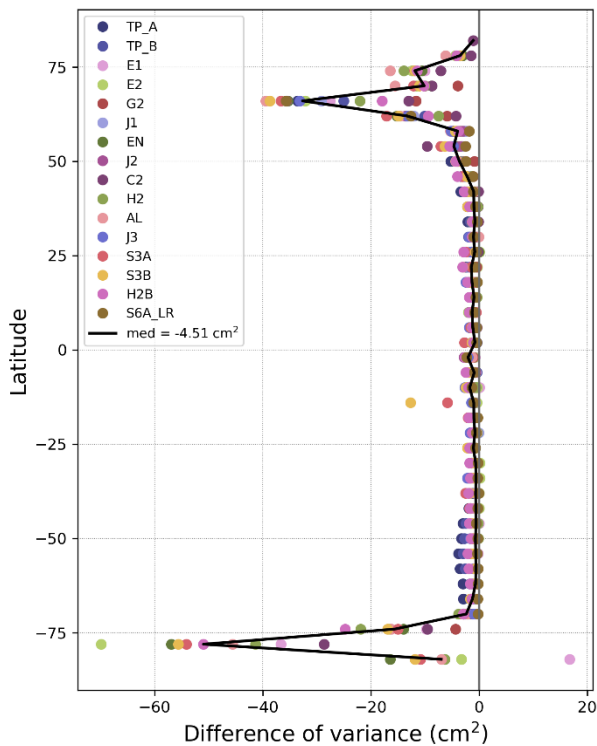
Figure 8 Difference of sea surface height variance at crossovers between DT-2024 - DT-2021 in function of coastal distance for each mission.

3.5 Polar improvements

Figure 9 shows that the most significant improvements are observed in the polar regions. These gains are primarily driven by
430 the updated ocean tide model (see Sect. 2.4.1) and by the contribution of high-latitude coverage missions, as the reference
satellite orbit does not exceed 66° latitude. In the Arctic (north of 66° S), the median error reduction in sea surface height



(SSH) crossover variance reaches more than 6 cm^2 , corresponding to a 18% improvement in this region. In the Antarctic (south of 66°N), the median error reduction reaches more than 8 cm^2 , representing the largest regional improvement in this reprocessing, amounting to an 27% gain in this region. For missions such as E2, EN, S3B, S3A and HY-2B, error reduction 435 exceeds 25 cm^2 (50%) near 66°S . The polar spatial distribution of the differences in SSH cross-over variance as observed by polar missions such as AL or S3A is shown on Fig. B 1.



440 **Figure 9 Difference of sea surface height variance at crossovers between DT-2024 - DT-2021 in function of latitude for each
coverage and precision mission.**

4 Cross-calibration methodology

In the previous section, we analyzed the SSHA error variance reduction focusing on mesoscale capabilities, mainly measured 445 at cross-overs. By design cross-overs are limited to errors with periods shorter than 10 days (see Sect 2.1). Another goal of this Level-2P/3 products is to provide consistent ocean topography measurements suitable to address climate science questions. In this section we describe how DT-2024 secures a seamless continuity of sea level measurements from 15 missions over 30 years, while preserving an unadulterated climate record.

We apply a four-step process cross-calibration process:



450 i) *pre-calibration*: well-documented instrumental effects are corrected on both reference and coverage missions. A correction is applied only for known and explained error sources for which an analytical or empirical correction is available in the peer-reviewed literature. This step intends to remove relatively simple error sources with analytical models.⁷

455 ii) *alignment of reference altimeters*: all reference altimeters (TOPEX and Jason series) are aligned with respect to Sentinel-6 MF (LR mode), which acts as an anchor. This alignment is small and straightforward thanks to tandem phases between subsequent reference altimeters. The tandem phase cancels out ocean variability in the cross-mission differences, which allows a precise estimation of the offsets, as well as good description of the MSL uncertainty error budget (the offset uncertainty is a significant item described by Guérou et al, 2023).

460 iii) *alignment of coverage missions* with respect to the combined reference record through the estimation of global time-invariant biases. This step intends to mitigate the time-invariant error sources of coverage missions, and to yield a crude alignment of static errors. Contrary to the previous step, the empirical models used for coverage missions are not always in peer-reviewed papers, but also from conference proceedings. This is acceptable because coverage missions do not control the climate time series of the DT-2024 dataset (see step iv below).

465 iv) *dynamical calibration of coverage missions on the reference altimeters*: this step mitigates high-frequency errors from precise orbit determination, barotropic tides and DAC model residuals, as well as instrumental drifts and biases in coverage missions. This is done using the climate-oriented altimeters as a reference. The first calibration mechanism uses the methodology of Le Traon and Ogor (1998) and the second calibration mechanism reduces residual long wavelength errors (Dibarbour et al, 2011). Note that after this calibration step, all satellites will exhibit climate MSL that is aligned, by construction, with the unadulterated MSL of reference altimeters. Any discrepancy from the radar processing, radiometer or geophysical models will be strongly reduced by this calibration. To that extent, the calibration process makes it possible to combine the extreme stability of reference 470 climate altimeters with the massive coverage of the other 10+ satellites.

After this process, subsequent reference altimeters provide a stable, consistent and seamless record that is trustworthy for climate indicators. Coverage and precision missions are also globally aligned with the reference record, with residual local discrepancies below 0.5 cm. Lastly, a core principle of this methodology is to preserve the independence of satellite 475 observations from exogenous data sources, such as in situ measurements or numerical model outputs.

⁷ Note that this processing step is extremely important because an uncontrolled calibration could affect the climate time series. For this reason, reference altimeters are generally not included in this processing step except if a peer-reviewed paper demonstrates that an error is understood and the analytical model is justified (e.g. bias reported by Cadier et al., 2024).



4.1 Precalibration

The cross-calibration process begins with mission-specific corrections targeting known anomalies to ensure the internal consistency of each satellite dataset. We describe here the set of corrections applied to the missions that required them, in order to ensure consistency and reliability across the dataset.

480

As demonstrated by Thibaut et al. (2021), MLE4 ranges on Jason-3 are impacted by a bias from cycle 57 to 85 related to echo centering changes following instrument resets (see Sect. 2.3). To mitigate this anomaly MLE4 ranges were unbiased using the Adaptive retracker ranges (0.8 mm bias).

485

Discontinuities between TOPEX-A and TOPEX-B were identified and corrected through cross-calibration techniques. Following the recommendations of Quet et al. (2023), a new bias estimation method was implemented, based on comparisons with the ERS-2 mission. This approach, which assumes both missions observe the same ocean over 10-day cycles and relies on the temporal stability of ERS-2, yielded a TOPEX-A/B bias of 3.4 ± 0.24 cm. This method preserves geophysical signals more effectively than previous constant or linear approaches and was adopted for the reprocessing of 490 L2P DT-2024 products. The inter-calibration of Poseidon-1 with TOPEX was achieved by deriving distinct empirical correction equations for each TOPEX side (A1, A2, and B). These equations were obtained by computing the sea level differences between Poseidon-1 and the corresponding TOPEX configuration using the Global Mean Sea Level (GMSL) method, thereby ensuring consistency across the altimeter time series.

495

The high-resolution (HR) altimeter data from Sentinel-6 MF (S6A) exhibits a wave-height-dependent bias when compared to J3 (Jason-3) or the low-resolution (LR) mode of S6A. To correct this effect, we apply a Look-Up Table (LUT) correction estimated from differences between S6A HR and J3. This approach effectively mitigates the wave-dependent bias, substantially improving consistency between the two missions. As a result of this correction, the agreement between S6A HR and S3A is also improved, with a reduction in crossover variance of over 0.5 cm² under strong wave conditions. Ongoing 500 investigations aim to identify and resolve the root cause of the wave-related bias, rather than relying solely on empirical LUT corrections. Despite the excellent resolution offered by S6A HR, remaining discrepancies with S6A LR and J3 hinders its use as a reference mission in delayed-time climate datasets. Nevertheless, we fully exploit its high-resolution capabilities in real-time applications, where such precision is most beneficial.

505

For CRYOSAT-2, following the recommendations of d'Apice et al. (2023), a correction of the pseudo time tag bias is applied in both LRM and SAR modes, along with a regional bias on SAR data to ensure continuity between the modes.



Finally, for HY-2A (Zhang et al., 2018), significant instrumental drifts and discontinuities are corrected by applying an empirical correction to ensure the consistency of the mission's trend with the Global Mean Sea Level (GMSL) and to 510 leverage the valuable mesoscale signals captured by the mission.

4.2 Alignment of reference altimeters

Although each reference mission is processed with state-of-the-art levels of accuracy and stability, small levels of unexplained discrepancies persist (remaining below the 1cm level), possibly stemming from processing residuals, or 515 instrumental discrepancies, precise orbit determination errors... Therefore, aligning subsequent high-precision datasets during their tandem phase is essential, as it enables sub-millimetric accuracy (better than 0.5 mm) and it ensures seamless continuity of the climate series.

To ensure a consistent mean sea level record, all satellite missions must be aligned to a common reference frame, requiring 520 stable orbits (Zawadzki and Ablain, 2016) and high-quality measurements. Tandem phases, where satellites fly 30s to 2 min apart from one another, provide near-identical ocean observations, making them ideal for detecting and correcting inter-mission 525 biases. These tandem periods allow for the detection and correction of regional biases related to latitude, wind, wave conditions, or orbital characteristics.

Long tandem phases can capture seasonal discrepancies relevant to climate studies. The quality of these reference missions 525 benefits significantly from extensive calibration and validation phases as demonstrated by each tandem outcome: TOPEX/Poseidon (Foster et al., 2025), Jason-1 (Bronner et al., 2016), Jason-2 (Roinard et al., 2022), Jason-3 (Flamant et al., 2024), Sentinel-6 MF (Cadier et al., 2025).

All reference missions are regionally aligned with the most recent reference mission using tandem phases. Sentinel-6 MF 530 (LR mode) is the regional reference for DT-2024, replacing Jason-3 used in the DT-2021 reprocessing. To ensure cross-mission consistency, we implement a stepwise cross-calibration approach: for each mission, we compute the mean bias relative to its successor. Unlike previous datasets, DT-2024 incorporates point-by-point corrections to enhance inter-mission consistency. Anomalous data points—especially near coasts or polar regions, where variability is high and representativity is low—are excluded to improve the spatial homogeneity of the maps. A Bessel filter is applied to better preserve and extrapolate spatial patterns, with the filter intensity adjusted according to the observed anomaly characteristics.

535

We observe differences between S6A LR and J3, which are now understood and explained. These biases include principally latitude-dependent differences and discrepancies to wave conditions. Each of these patterns has known origins:

- We can observe latitude-dependent differences, with two peaks around the equatorial band and around 40°S, in both J3 vs. S6A LR and TP vs. J1 shown on Fig. 10. This pattern is not present in the J1/J2 and J2/J3 tandem phases



540 because they all share the same anomaly. This artifact was shown to be caused by a truncation of the range measurements in the L2 data processing, i.e. a software bug (Cadier et al, 2025).

- C-band differences between S6A and J3 affect ionospheric corrections depending on wave height, but remain below 0.7 cm for SWH between 1 and 7 m (Cadier et al., 2025).
- At a second order (<2 mm/SWH), the S6A Ku band range is impacted by pulse-to-pulse correlation effects.
- A bell-shaped latitude bias between J3 and S6A is likely due to orbital effects (Courcol et al., 2024).
- In low wave conditions, S6A LR uses a more realistic approach for small waves, both in terms of values and noise.

545 All these differences are now well characterized, which is why we apply specific corrections to address the S6A/J3 bias. For example, since the improved small wave handling from S6A is not yet implemented in the reprocessing of J3, we aligned J3 with S6A LR using a time-invariant regional bias. The latitude-dependent discrepancy between S6A LR and J3 datasets was 550 used to correct J3 and subsequently applied to earlier missions (J2 and J1) to address similar anomalies. To preserve the precision of the equatorial anomaly, no smoothing was applied in this region. In contrast, smoothing was performed at other latitudes to ensure consistency and harmonization across datasets. The resulting S6A LR / Jason-3 bias map is shown on the right in Fig. 10 (right column). Regional biases enhance the consistency between the S6A LR and J3 missions for explained 555 differences. Note that all of these corrections will be a part of the next Level-2 standards and reprocessing (tentatively GDR version G).

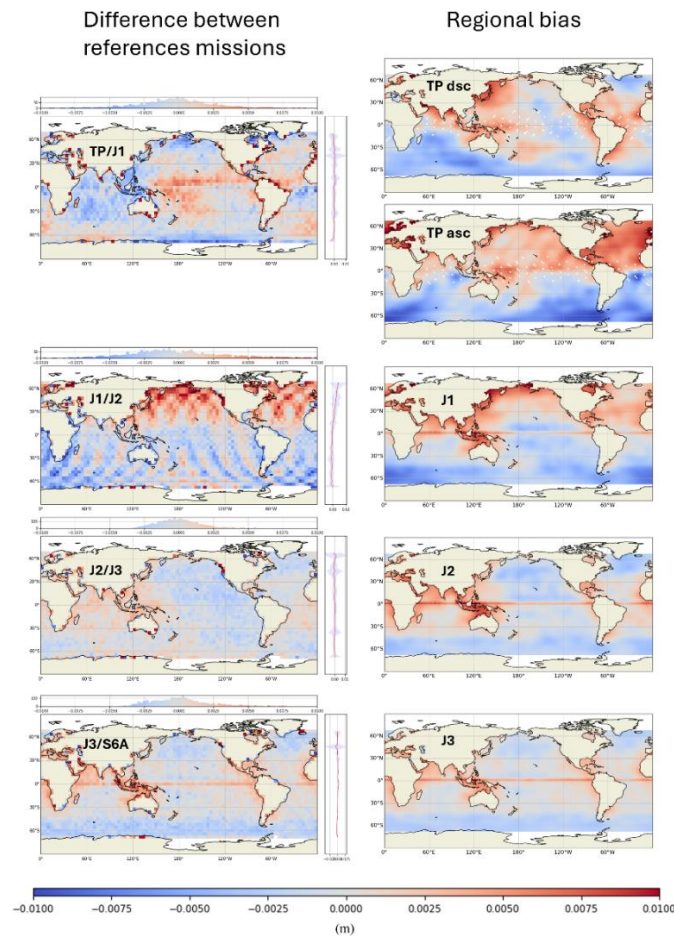
560 Jason-3 is almost a carbon copy of Jason-2 (hardware and ground processing). This coherence is reflected in the stability of their measurements with extremely small differences as shown on the Fig. 10 (left column). This stability and the lack of notable bias between them is desirable for ocean observation at climate scales. However, this consistency may hide common errors to both satellites (Cadier et al, 2024). Although minor discrepancies remain in the small-wave regime, they can be corrected by applying a constant regional bias. When added to the bias already applied to Jason-3, this additional correction allows Jason-2 to be aligned with the Copernicus Sentinel-6 MF (S6A) reference. The resulting adjustment applied to Jason-2 is illustrated in Fig. 10 (right column).

565 Differences between J1 and J2 are more challenging to interpret because J1 lost its GPS receiver before the tandem phase with J2, increasing the uncertainty associated with precise orbit determination (POD). The use of the new POE version F on J1 helps mitigate this impact. Significant north/south biases are observed with J2 as shown on Fig. 10 (left column), which can be corrected. The stripe-shaped artifacts from POD are clearly time-varying, so they are smoothed out of the J2/J1 bias map. Combined with other biases from J2 and J3, we aligned J1 with S6A LR, with the resulting bias shown in Fig. 10 (right 570 column).



Regarding TP/J1 differences, the latitude biases observed between J3 and S6A are mirrored at the equator and 40° south (Fig. 10 left column). Thus, we applied the latitudinal bias as the opposite from those applied on the Jason series to address the anomaly caused by the truncation of the range differently on ascending and descending passes only on the Jason series, 575 as observed in (Cadier et al, 2024). The bias is significant between ascending and descending passes between TP and J1, so we correct them independently. Combined with other biases from J1, J2, and J3, we aligned TP with the S6A LR regional reference (Fig. 10 right column).

Thanks to the reference orbit and the subsequent tandem phases, we can observe similarities between S6A and TP, even 30 580 years later, apart. and deduce anomalies in the Jason series with an accuracy of 5 mm in amplitude and a width of only 5° in the equatorial band. Through the application of these biases, all the reference missions are regionally aligned with S6A LR to ensure the regional continuity of the missions over a span of 30 years.



585 **Figure 10** Difference between the SSHA of subsequent reference altimeters (left) and offset corrections applied (right). Note that for J3 vs. S6A, the dynamic atmospheric correction is not applied. All the maps are centered on the mean value and calculated on the full tandem phases.



590 The next step is a global calibration aimed at establishing a unified reference system for all missions, facilitating the creation of consistent Global Mean Sea Level (GMSL) records. For both reference and auxiliary missions, GMSL time series are derived from Sea Surface Height Anomaly (SSHA) data. These are first averaged over $1^\circ \times 3^\circ$ latitude-longitude boxes and 10-day intervals (Henry et al., 2013), matching the orbital cycle of reference missions. A global weighted mean is then computed, accounting for both latitudinal area differences (via cosine weighting) and ocean/land coverage fraction. By
595 convention, the baseline year is set to 1993, where the TOPEX GMSL is zeroed. Successive reference missions (J1, J2, J3, S6A) are cross-calibrated during their tandem phases. The DT-2024 approach notably utilizes the entire tandem phase, reducing both noise and seasonal bias (Guérou et al., 2023), thereby enhancing the robustness of the GMSL reference compared to previous processing.

600 This reprocessing is particularly important because it includes the reprocessing of some reference missions. These reference missions form the foundation for the global mean sea level (GMSL) and are crucial for CMEMS products. These reference missions are essential for reliable climate monitoring and the accurate assessment of sea level rise reaching 4.07 mm/yr since the last 10 years (Fig. 11). As mentioned in Sect. 2.3, TOPEX A mission currently do not appear on global mean sea level trend analysis due to ongoing studies aimed at enhancing the retracking calibration process. Uncertainties and error budget of
605 the GMSL are quantified by Quet et al. (2025).

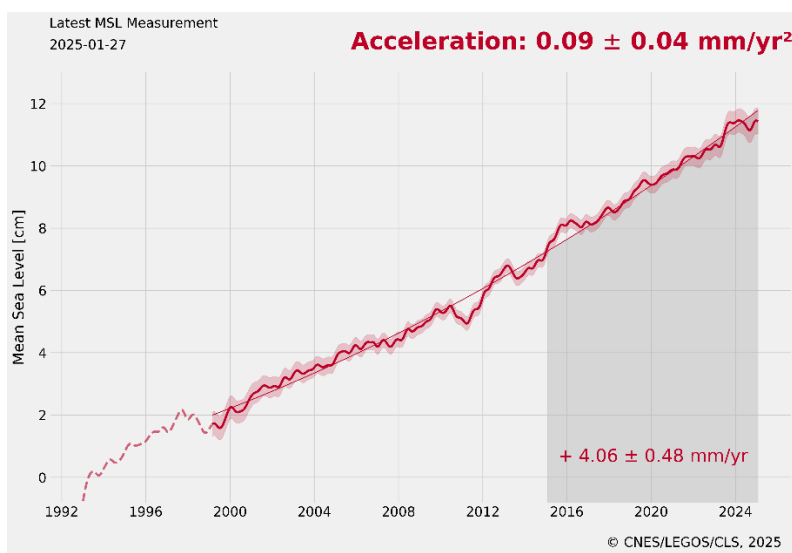
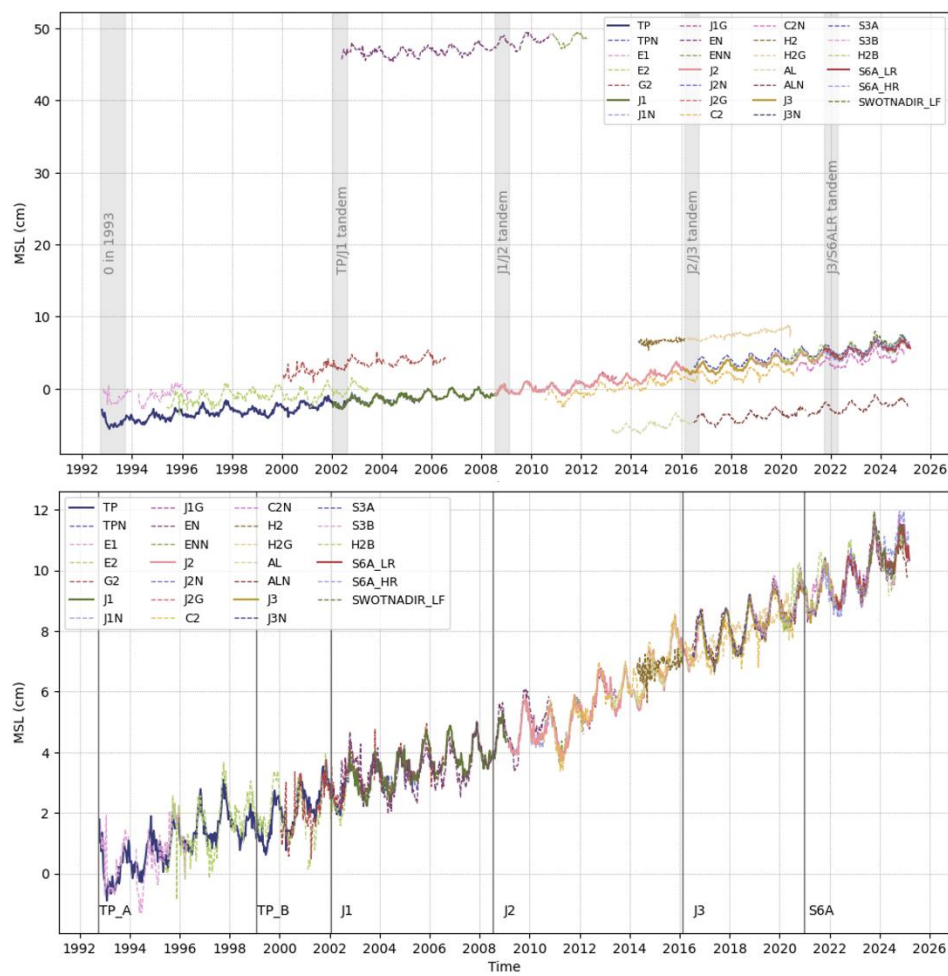


Figure 11 global mean sea level on reference missions with DT-2024 version corrected from Glacial Isostatic Adjustment (+ 0.3 mm/year)



610 4.3 Alignment of coverage missions

Coverage and precision missions are calibrated against the climatic reference established by the reference missions. Some of the coverage missions (the older ones in particular) may contain significant instrumental drifts, processing drifts and offsets, so we estimate the time-invariant bias between each of them and the MSL from reference altimeters. This estimation is performed through a least-squares minimization applied to spatially weighted 10-day averages of Sea Level Anomalies 615 (SLA). The spatial weighting accounts for both latitude and proximity to coastlines, reflecting the varying data density across regions. The 10-day averaging period corresponds to the repeat cycle of the reference missions, ensuring temporal consistency in the comparison. This alignment over the GMSL time series is illustrated in Fig. 12, starting from the top and applying the biases to the figure on the bottom. All the missions show a consistent sea level rise, albeit not on par with the stringent accuracy of reference altimeters.



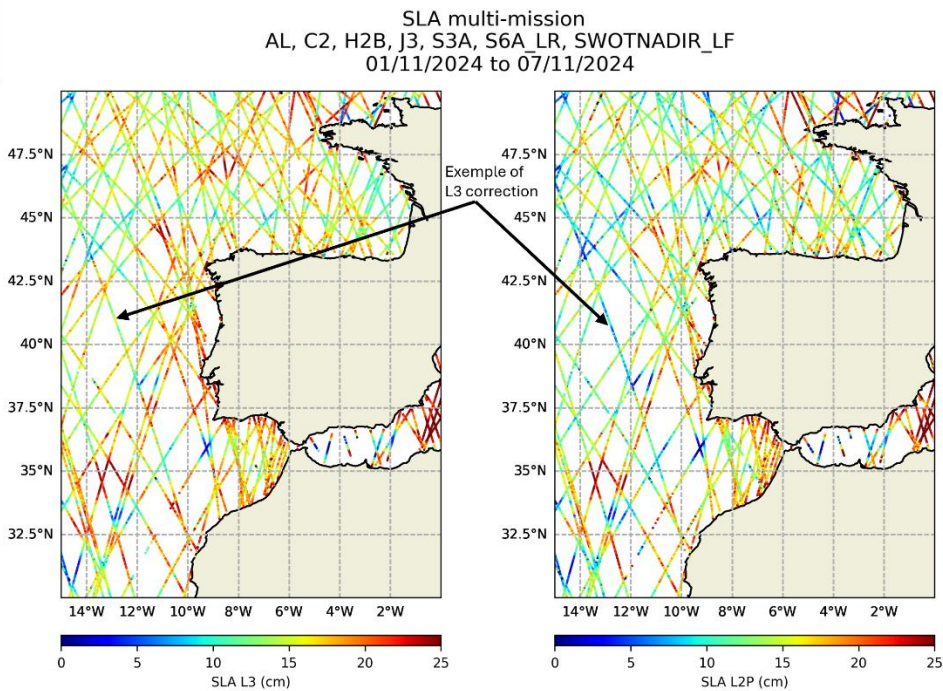
620 Figure 12 Sea Level Anomaly before (top) after alignment (bottom)



4.4 Dynamical calibration of coverage missions on the reference altimeters

Despite this alignment on a common MSL derived from the reference altimeters, the measurements from different altimeters
 625 are not always coherent at large regional scales due to time-varying, geographically correlated error residuals (e.g. instrumental, processing, geophysical models, precise orbit determination).

To address this, coverage missions are processed using a so-called Level-3 multi-mission calibration (Le Traon and Ogor,
 1998), which minimizes crossover differences between the reference and secondary missions. Leveraging the high-precision
 630 orbits of the TOPEX/Jasons/Sentinel-6 series, most reference-related errors are mitigated. Then the last calibration step
 handles zero-mean high-frequency residual errors (e.g. tides or DAC residuals, HF precise orbit determination regional
 biases per pass). The so-called long wavelength error correction (Dibarboore et al, 2011, or the variant from Ubelmann et al.
 2021): during the Level-4 mapping process with an optimal interpolator, the local biases of each along-track SLA
 observations are estimated and mitigated. This empirical correction reduces geographically correlated errors across adjacent
 635 tracks from different sensors and mitigates residual high-frequency signals. Because the process has a zero mean by
 construction, it will not affect previous calibration steps. The output of this final calibration process is one Level-3 along-
 track dataset for each satellite of the constellation shown on Fig. 13.



640 **Figure 13** Sea level anomaly from the 01/11/2024 to 07/11/2024 for mission AL, C2, H2B, J3, S3A, S6A (LR) and SWOT (nadir) at
 Level-2P processing step on the left and at Level-3 processing step on the right.

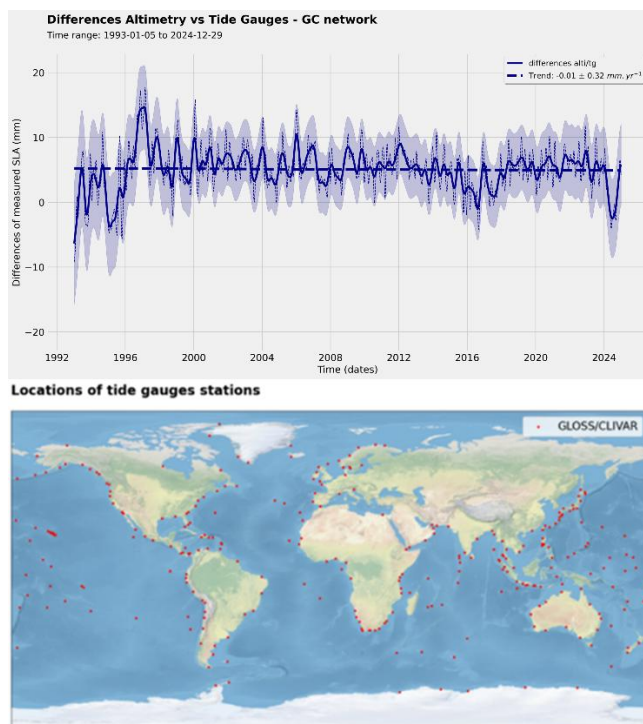


5 Validation against in-situ data

In order to verify that the calibration process described in previous section does not alter the altimetry mean sea level series, we performed a sanity check comparison of the DT-2024 Level-2P data with completely independent in-situ tide gauge measurements, focusing on reference missions to assess the dataset's stability, albeit limited to a relatively small set of locations with tide gauges (Fig. 14). The comparison exhibits no significant drift, with a trend of 0.01 mm/year and background noise with a STD of a few millimeters only: both times series are very consistent in their observation of the local sea level variability in coastal zones.

650 Some differences are visible before 1999, on TOPEX side A: they could be caused by the reprocessed L2 input product. The previous iteration of TOPEX-A data used an empirical correction derived from the 3 independent assessment methods. The new TOPEX-A dataset may require a similar correction. Additionally, the differences between DT-2024 and the in-situ is slightly larger around 2016: this might be related to a drift from a Jason radiometer (Barnoud et al., 2023).

655 The comparison with tide gauge measurements demonstrates the robustness of DT-2024 in coastal areas. This close agreement reinforces confidence in its ability to accurately monitor sea level anomalies, which are essential for assessing surface currents in these regions.



660 **Figure 14** Sea level anomaly differences between Altimetric reference missions and Tide gauges from GLOSS/CLIVAR network (top). Location of tide gauges used for the comparison (bottom)



6 Past and future evolutions

6.1 Historical context: how does DT-2024 compare with previous upgrades?

The impact of the DT-2024 reprocessing has been quantified in Sect. 3. But how does this gain compare with previous reprocessing? The gains in SSH crossovers (Fig. 15) illustrate the overall improvement driven by each subsequent 665 reprocessing (color changes). The very first reprocessing on TOPEX, over 15 to 20 years ago, resulted in a massive 30% improvement. After 2010, all subsequent reprocessing reached an asymptote of 5 to 10% per reprocessing. In this context, the DT-2024 reprocessing brings improvements of a similar magnitude to those seen in the last 15 years, with around a 6% 670 gain in variance at SSH crossover for all missions (Sect. 3.2). The improvements from DT-2024 stack up with similar gains from previous reprocessing campaigns, highlighting a continuous progress made in satellite altimetry with every reprocessing cycle since the nineties.

The remaining SSH crossover errors are over 4.2 cm in the open ocean⁸: this number is the sum of the ocean variability in 0 to 5 days, and altimetry error variability over the same time span. Altimetric errors are increased in regions of strong active 675 mesoscale dynamics (Vergara et al. 2023) (e.g. western boundary currents), continental shelf, coastal regions, and the presence of sea-ice (latitude >50°). By excluding these areas, the green contours in Fig. 15, the median error at crossover difference is of the order of 3.6 cm (assuming the error is random and distributed evenly on the ascending and descending passes).

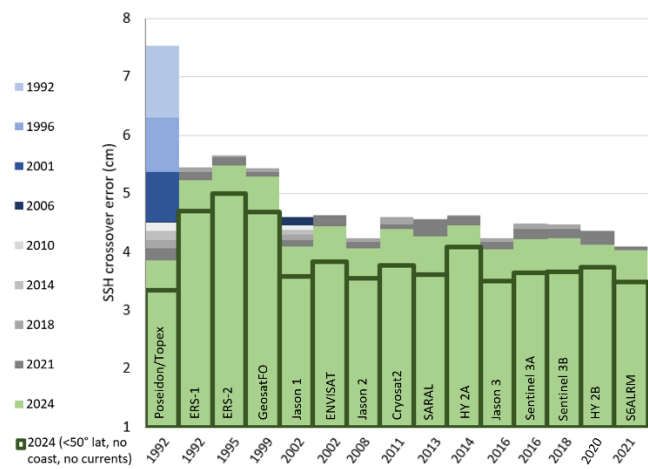


Figure 15 Errors at sea surface height crossovers for each mission for each general reprocessing in the last 30 years. Source of data before 2018 (Faugere et al. 2006 ; and Labroue et al. 2018)

⁸ Except for ERS and GFO: these old satellites have various documented sources of errors such as more random noise, more POD errors, which are not entirely mitigated by the Level-3 calibration process. For reference, that is approximately 3 cm RMS more than other satellites.



6.2 Toward future reprocessing

The state-of-the-art in altimetric corrections and processing algorithms is continuously evolving, driven by ongoing research and the accumulation of long-term observational records. Given the complexity of the reprocessing framework, spanning over 100 years' worth of data from 15 satellites, it takes approximately 3 years or more between the start of a multi-mission
685 reprocessing cycle (e.g. R&D studies, standard definition) and the dissemination of the final Level-3/Level-4 products.

During this 3-year period, new algorithms and models may emerge, prompting a reassessment of whether their integration is warranted or premature. In this context, several promising research developments have been identified but they were either too late for the DT-2024 timeline, or lacking user-oriented evaluations (e.g. uncertainty on MSL drift, untested robustness in
690 the coastal or polar ocean). They could be tentative candidates for future delayed-time (DT) reprocessing. While the list is too long for this paper, we can illustrate with a few representative examples:

- *The 3-parameter sea state bias model.* In addition to the classical inputs (significant-wave height and surface wind speed), the algorithm adds a third input variable: the wave period, based on interpolated wave model outputs. This method has been published and it exhibits good potential to improve mesoscale accuracy. However, it opens up a series of questions about the climate stability of wave model parameters, or the sea-state bias itself. When the DT-2024 standards were defined, we lacked evidence on this change, so it was ruled out as a precaution. This choice will be revisited in a future DT-202x iteration.
- *The so-called adaptive retracking algorithm* exhibits a significant reduction in SSH crossover variance compared to MLE4 (0.52 cm², i.e. 5% of the total SSHA variance, and 17% of the variance of scales less than 100 km). However, its wave-dependent behavior differs from that of MLE4 retracking, with implications on sea-state bias models, and regional and global MSL. Without a new coherent suite of corrections, what is gained in precision could be lost in accuracy or stability. Lacking more evidence at the time DT-2024 was defined, the new algorithm was ruled out in order to preserve the consistency with the TOPEX/Jason series based on the MLE4 retracking. This choice will be revisited in a future DT-202x iteration.
- Lastly, several ongoing studies aim to improve global mean sea level trend estimates by addressing known instrumental drifts, such as the *TOPEX-A range drift* and *radiometer drifts on the Jason missions*. Should these investigations demonstrate consistent improvements when compared to independent reference datasets, their corrections may be incorporated into future reprocessing cycles to enhance the accuracy and stability of the altimetric climate data record.



These examples illustrate that the DT-2024 was a rigorous and careful approach to reprocessing, balancing scientific
715 innovation with the need to maintain the integrity and homogeneity of long-term sea level observations.

The DT-2024 Level-2P dataset is available to users for all the altimeter missions on AVISO+
(<https://doi.org/10.24400/527896/a01-2025.004>). The Level-3 and Level-4 counterparts are available on the Copernicus
Marine Service catalogue (<https://marine.copernicus.eu>) and C3S (<https://cds.climate.copernicus.eu/>).

720 7 Conclusion

The DT-2024 satellite altimetry reprocessing is a massive endeavor spanning over more than a 100 years' worth of data, from 3 decades, 15 satellites, and 5 climate reference altimeters. In our effort to enhance the user-oriented "reliability" of sea level measurements, we focus on the refinement of altimetry satellite standards (radar processing algorithms and geophysical models) and on the cross-mission consistency. Reliability is here treated as a multi-dimensional spectrum
725 encompassing coverage, precision, accuracy, and stability. These four pillars are essential, not only to capture short-term ocean variability (large and small eddies) for the open, coastal and polar oceans, but also to detect seasonal and long-term climate signals such as global mean sea level rise.

The diversity of so many algorithms and usages makes it critical to control the overall consistency of the system: to question
730 the differences between satellites that can be separated by decades, to preserve not just the data and the code but also the knowledge of each mission history and properties, to question the relevance of new algorithms for multiple user communities, and to mitigate the discrepancies between so called 'coverage and precision altimeters and 'climate reference altimeters'. This effort is crucial in the development of DUACS (Data Unification and Altimeter Combination System) to serve the wide range of research and operational users from the Copernicus Marine and Climate Changes Services (Pujol et
735 al, 2024; Cazenave et al, 2019). All this work is not carried out in a vacuum: it is a convergence framework of the collaborative efforts of multiple agencies on their satellites, and the research from many scientists from remote sensing and oceanography communities (e.g. members of the Ocean Surface Topography Science Team).

By extending the time series, adding new satellites, and upgrading the precision of altimetry products while ensuring cross-
740 mission consistency, we enable the study of finer-scale phenomena and novel oceanographic processes. In polar regions, the most significant improvements are observed, with large crossover variance error reductions: a massive 7.7cm² in the Arctic (27% of the regional SSH variance), and 5.9cm² (18%) in the Antarctic. These gains enhance the monitoring of freshwater fluxes and large-scale circulation patterns around ice-covered areas, where in situ observations remain sparse (Sallée et al, 2025). In coastal regions, DT-2024 shows a 5.6cm² error reduction in crossover variance (17%), largely due to the improved
745 tidal correction from FES22. These improvements will enhance the monitoring of sea level trends, storm surges, and coastal



processes such as upwelling, which are critical for ecosystem dynamics and coastal risk assessment. In open ocean, the DT-2024 reprocessing introduces new geophysical corrections that reduce the error of the sea surface height variance at SSH crossovers by 1.2cm² (6%). These gains mainly originate in the FES22 ocean tide model (70% of the variance reduction), new input Level-2 reprocessing (TOPEX/Poseidon in particular), the new dynamical atmospheric correction model TUGO 750 forced by the ERA5 reanalysis, the hybrid mean sea surface CLS/DTU/SIO H23, and updated instrumental corrections.

Securing the stability of sea level measurements is crucial for accurate climate monitoring and analysis (Cazenave et al, 2019). To support climate applications, the DT-2024 definition was rigorous with new algorithms that might change the trends of the multi-mission dataset (any change has to be traced and explained). To ensure the accuracy and consistency of 755 sea level measurements over time, we align all coverage and precision missions on a unified reference frame, based on the reference climate altimeter series. The reference altimeters are extremely consistent with one-another thanks to their so-called tandem phases (formation flight) although we compute small static offsets between subsequent reference altimeters to improve the continuity (and to estimate the uncertainty of the transition between reference altimeters). Independent comparisons with independent in-situ tide gauges yield an agreement within 0.01 mm/year in the regions where tide gauges 760 are located. They also highlight possible weaknesses (TOPEX Level-2 reprocessing, and Jason microwave radiometers) that might need revisiting in a future DT-202x reprocessing. The new DT-2024 dataset exhibits a global mean sea level rise of 4.07 mm/year for the last decade.



Appendix A

Figure A 1 lists the standards used in the DT-2021 reprocessing. The most recent updates are highlighted in dark grey, while
 765 the standards that have remained unchanged since the first reprocessing in 2010 are shown in very light grey.

MISSION	Poseidon	Topex	Jason 1	Jason 2	Jason 3	ERS-1	ERS-2	ENVISAT	Geosat FO	SARAL	Cryosat 2	HY 2A	HY 2B	Sentinel 3A	Sentinel 3B	Sentinel6A/JasonCS													
															LRM	SAR													
L2 version	MGDR	MGDR	GDRE	GDRD	GDRF	OPR		RA2/MWR V3.0	OPER	GDRF	BC	Unknown		BC004	FO6/F07(>65)/F08(>83)/FO9(>122)														
RETRACKING	On board tracker LRM	On board tracker LRM	MLE4	MLE4 LRM	MLE4	OPR LRM		MLE3 (OCE-1) LRM	Onboard tracker LRM	MLE4 LRM	SAMOSA2.3 SAR/LRM	MLE4 LRM		SAMOSA	LRM MLE4/Numer SAMOSA SAR ical (>83)														
ORBIT	GSFC std 18	POE-E	POE-F		Reaper		POE-E	GSFC	POE-F	POE-F	POE-F	POE-D	POE-F	POE-F	POE-F														
IONOSPHERIC CORRECTION	DORIS	Filtered dual frequency [7]	Filtered dual frequency [7]	Filtered dual frequency [7] (SSB C band)	NIC09 [11]	GIM [8]		Filtered from L2 (SLOOP) ; c>65 GIM [8]		GIM [8]		GIM [8]		Filtered from L2		Filtered dual frequency altimeter range from L2 LR													
SEA STATE BIAS	BM4	Non parametric [12]	2D J1 Non parametric [15]	2D J2 Non Parametric [13]	Non parametric from J2 [13] & c>170 [18] J3 GDRF	BM3 [6]	Non parametric [9]	2D EN Non parametric [16]	Non parametric [12]	Non parametric [17]	Non parametric [17] BC	Non Parametric [14]	L2 product	Non parametric [13]	Non parametric from [18] J3 GDRF														
WET TROPOSPHERE	GPD+ [5]		JMR radiometer	AMR radiometer	AMR Radiometer	GPD+ [5]		MWR radiometer	Radiometer & HRES model	Neuronal Network (5 entries) V4	GPD+ [5]	HRES model	HRES model & radiometer (>c42)	MWR 3 radiometer	Radiometer HR/LR														
DRY TROPOSPHERE	ERAS (1-hour) model based																												
DYNAMICAL ATMOSPHERIC	TUGO High frequencies forced with reanalysed ERA 5 pressure and wind field + inverse barometer Low frequencies			TUGO HF (ERA 5 pressure/ wind); >02/2016 MOG2D HF (ECMWF analysis pressure / wind) inverse Barometer LF	MOG2D HF (ECMWF analysis pressure /wind) [1] + inverse Barometer LF	TUGO High frequencies forced with analysed ERA 5 pressure and wind field + inverse barometer Low frequencies				TUGO HF forced with analysed ERA 5 pressure and wind field; >02/2016 MOG2D HF (ECMWF analysis pressure / wind) + inverse barometer LF		MOG2D High frequencies forced with analysed ECMWF pressure and wind field [1] + inverse barometer Low frequencies																	
OCEAN TIDE	FES 2014 B [2]																												
INTERNAL TIDE	HRET v8.1 tidal frequencies: M2, K1, S2, O1 [19]																												
POLE TIDE	Model Desai 2015 [4] Mean Pole Location 2017																												
SOLID TIDE	Elastic response to tidal potential [3]																												
MEAN SEA SURFACE	Composite (SCRIPPS,CNES/CLS15,DTU15)																												
															STD 21	STD 18	STD 14	STD 10											

Figure A 1 Sea level standards table for DT2021. Gray colors show when each standard changed since DT2010. Sources [1] Carrère and Lyard, operational version 3.2.0, 2003 [2] (L. L. Carrere 2016) [3] (Cartwright D. E. and Taylor R. J. 1971); (Cartwright D. E. and Edden A. C. 1973) [4] (Desai S. 2015) [5] (Fernandes M J. 2016) [6] (Gaspar 1994) [7] (Guibbaud 2015) [8] (Ijima 1999) [9] (Mertz 2005) [11] (Scharroo 2010) [12] (N. L. Tran 2010) [13] Tran, 2012a [14] Tran, 2012b [15] (N. Tran, SSB Activity 2015) [16] (Tran N. 2017) [17] (N. Tran, "ESL Cryosat-2: Tuning activities(wind speed and SSB)" 2018) [18] Tran, 2020, [19] (Zaron 2019)



Appendix B

The DT-2024 reprocessing brings considerable improvements on the polar areas, visible on the SSH cross-over variance
775 difference as shown by polar missions like AL or S3A on Fig. B 1.

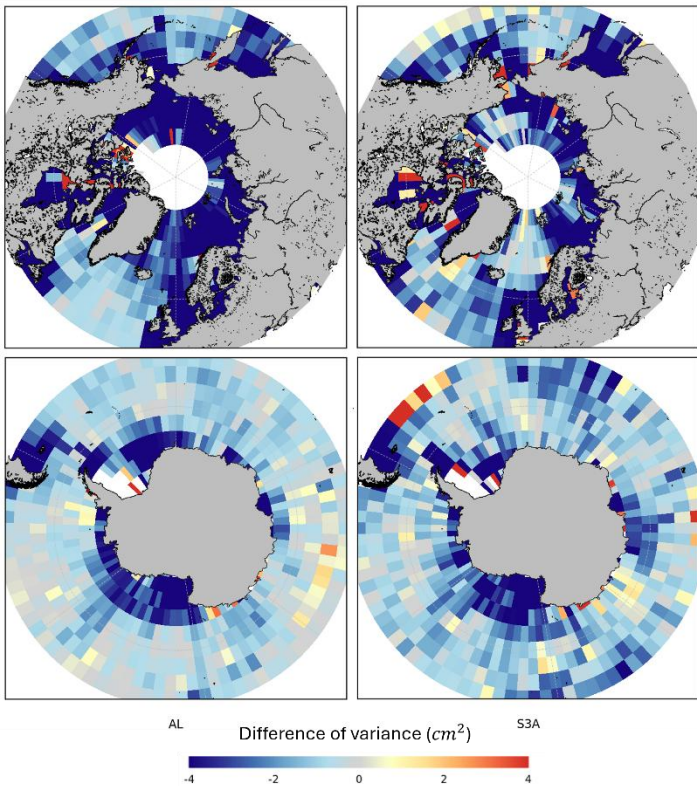


Figure B 1 Sea surface height crossover variance between standards 2024 minus standards 2021 for missions AL (left) and S3A (right)

Data availability

780 The DT-2024 Level-2P dataset is available to users for all the altimeter missions on AVISO+. The Level-3 and Level-4
counterparts are available on the Copernicus Marine Service catalogue (<https://marine.copernicus.eu>) and C3S (<https://cds.climate.copernicus.eu/>):

- Level-2P Global Ocean Multi-Year product: <https://doi.org/10.24400/527896/a01-2025.004>
- Level-3 Global Ocean Multi-Year product: <https://doi.org/10.48670/moi-00146>
- Level-3 European Seas Multi-Year product: <https://doi.org/10.48670/moi-00139>
- Level-4 Global Ocean Multi-Year product: <https://doi.org/10.48670/moi-00148>
- Level-4 European Seas Multi-Year product: <https://doi.org/10.48670/moi-00141>
- Level-4 Climate-focused product: <https://doi.org/10.48670/moi-00145> or [10.24381/cds.4c328c78](https://cds.climate.copernicus.eu/cdsapp#!/dataset/dt-2024-climate?tab=description)



Author contributions

790 CK, ML, YP, and CR conducted the studies, data processing, validation, and manuscript writing. VQ and FO created the GMSL images and performed the comparisons with tide gauges. GD, MIP, PP, and SP contributed to the writing. GD, ID, CNL, TG and FBC participated in the development and successful execution of the project.

Competing interests

795 The authors declare that they have no conflict of interest.

Acknowledgements

This work was supported by the Centre National d'Etudes Spatiales (CNES), the European Organisation for the Exploitation of Meteorological Satellites (EUMETSAT), the Copernicus Marine Service, the Copernicus Climate Change Service and the Copernicus Program.

800 References

Ablain, M., Jugier, R., Zawadzki, L., Taburet, N., Cazenave, A., Meyssignac, B., Picot, N., "The TOPEX-A drift and impacts on GMSL time series." *OSTST meeting*. Miami, Florida, 2017.

Andersen, O. B., Rose, S. K., Abulaitijiang, A., Zhang, S., & Fleury, S. "The DTU21 global mean sea surface and first evaluation. *Earth System Science Data*," Vols. 15(9), 4065–4075. <https://doi.org/10.5194/essd-15-4065-2023>.

805 2023.

Aulicino, G., Cotroneo, Y., Ansorge, I., Van den Berg, M., Cesarano, C., "Sea surface salinity and temperature in the southern Atlantic Ocean from South African icebreakers, 2010–2017." *earth system science data* 10 (3), 1227-1236, <https://doi.org/10.5194/essd-10-1227-2018> (2018).

Bignalet-Cazalet, F., Picot, N., Desai, S., Scharroo, R., and EGIDO, A. "Jason-3 Products Handbook." 2021.

810 Bronner E., N. Picot, J-D. Desjonquieres, S. Desai, J. Hausman, L. Carrere, N. Tran. *Jason-1 Products Handbook*. handbook, https://aviso.altimetry.fr/fileadmin/documents/data/tools/hdbk_j1_gdr.pdf, AVISO, 2016.

Brown, S., Islam, T. "Jason-3 GDR Calibration Stability Enabled by the Cold Sky Maneuvers." *OSTST*. 2017.

Buchhaupt, C. "Model Improvement for SAR Altimetry." *Ph.D. Thesis*, 2019.

815 Cadier, E, Bracher, G , Maraldi, C , Courcol, B , Prandi, P , Kocha, C. , Pujol, M. , Bignalet Cazalet, F. "Equatorial band : Topex was right from the start. An upcoming correction of Jasons and Swot Nadir ground segments." *"30 Years of progress in radar altimetry" symposium*. Montpellier, 2024.



Cadier, E., Courcol, B., Prandi, P., Quet, V., Moreau, T., Maraldi, C., Bignalet Cazalet, F., Dinardo, S., Martin Puig, C., Donlon, C. "Assessment of Sentinel-6MF low resolution numerical retracker over ocean: Continuity on reference orbit and improvements." *Advances in Space Research* 75, 30-52, doi:10.1016/j.asr.2024.11.045., no. 1 (2025).

820 Carrere, L. "Improving the geophysical corrections for altimeters and SWOT tides and DAC." *OSTST*. 2023.

Carrere, L., "A new barotropic tide model for global ocean: FES2022." *OSTST*. 2022.

Carrere, L., Lyard, F., Allain, D., Cancet, M., Picot, N., Guillot, A., Faugere, Y., Dupuy, S., Baghi, R. "Final Version of the FES2014 global ocean tide model which includes a new loading solution." *OSTST*. Vol. https://meetings.aviso.altimetry.fr/fileadmin/user_upload/tx_ausyclsseminar/files/Poster_FES2014b OSTST_2016.pdf. La Rochelle, 2016.

825 Cartwright D. E. and Edden A. C. "Corrected Tables of Tidal Harmonics." *Geophysical Journal International*, September 1973: 253–264.

Cartwright D. E. and Taylor R. J. "New Computations of the Tide-generating Potential." *Geophysical Journal International*, 1971: 45-73.

830 Cazenave, A., Hamlington, B., Hrwath, M. Barletta, V., Benveniste, J., Chambers, D., Dool, P., Hoog, A., Legeais, J.-F., Merrifield, M., Meyssignac, B., Mitchum, G., Nerem, S., Pail, R., Palanisamy, H., Paul, F., Von Schuckmann, K., Tompson, P. "Observational Requirements for Long-Term Monitoring of the Global Mean Sea Level and Its Components Over the Altimetry Era." *Sec. Ocean Observation* 6, <https://doi.org/10.3389/fmars.2019.00582> (2019).

835 Charayron, R., Schaeffer, P., Ballarotta, M., Delepoule, A., Laloue, A., Pujol, M.-I., and Dibarboure, G. "Blending data from SWOT KaRIn science phase and 30 years of nadir altimetry to improve Mean Sea Surface models." *EGU General Assembly*. Vienna, Austria: EGU25-8570, <https://doi.org/10.5194/egusphere-egu25-8570>, 2025.

Courcol B., L. Rinchiuso, V. Quet, P. Prandi, F. Bignalet-Cazalet, A. Couhert, J. Moyard, S. Houry, F. Mercier. "Impact of POE-G orbits on Sentinel-6 MF and Jason-3 altimetric performances." *30yrsPRA*. 2024.

840 D'Apice G., Amarouche L., Prandi P., Tran N., Gayrard N. "CryoSat-2 Ocean Processor (COP) Baseline D: Changes in the processing chain and CalVal activities." *CryoSat-2 Quality Working Group*. 2023.

Desai S., Wahr J., Beekle B., "Revisiting the pole tide for and from satellite altimetry." *Journal of Geodesy*, 2015: 1233–1243.

Dibarboure, G., Pujol, M. I., Briol, F., Traon, P. L., Larnicol, G., Picot, N., Mertz, F., Ablain, M. "Jason-2 in DUACS: Updated system description, first tandem results and impact on processing and products." *Marine Geodesy* 34(3-4), 214-241, <https://doi.org/10.1080/01490419.2011.584826> (2011).

845 Dinardo, S., Maraldi, C., Cadier, E., Rieu, P., Aublanc, J., Guerou, A., Boy, F., Moreau, T., Picot, N., Scharoo, R. "Sentinel-6 MF Poseidon-4 radar altimeter: Main scientific results from S6PP LRM and UF-SAR chains in the first year of the mission." *Advances in Space Research* 73, 337–375, <https://doi.org/10.1016/j.asr.2023.0>, no. 1 (2023).



850 E.D, Zaron. *Baroclinic Tidal Sea Level from Exact-Repeat Mission Altimetry*. Vol. 49. J.Phys. Oceanogr., 2019.
ECMWF. “47r3 HRES scorecard.” 2024.

Escudier, P., et al. "Satellite radar altimetry: principle, geophysical correction and orbit, accuracy and precision." *CRC Book on satellite altimetry*, 2017.

EUMETSAT. “Sentinel-3B USO sign correction.” 2021.

855 Faugere, Y., Dorandeu, J. Lefevre, F., Picot, N., Femenias, P. “Envisat Ocean Altimetry Performance Assessment and Cross-calibration.” *Sensors* 6(3), 100-130, <https://doi.org/10.3390/s6030100> (2006).

Fernandes M J., Lázaro C. “GPD+ Wet Tropospheric Corrections for CryoSat-2 and GFO Altimetry Missions.” *Remote Sensing*, 2016: 851.

Fernandes, M. J., Vieira, T., Lázaro, C., Vasconcellos, B., Aguiar, P.,. “Improving Sentinel-3 Altimetry Data With GPD+ Wet Tropospheric Corrections.” *AGU*, August 2024: Volume11, Issue8, <https://doi.org/10.1029/2024EA003536>.

860 Flamant B., Coquelin J., Bignalet Cazalet F. “Jason-3 In-flight performance.” *30 Years of Progress in Radar Altimetry Symposium*. Montpellier: poster 142, <https://az659834.vo.msecnd.net/eventsairwesteuprod/production-nikal-public/1f1c28a652e94ae8834e5adf3fbc3d4f>, 2024.

Forster Linda, Desjonquères Jean-Damien, Talpe Matthieu, Desai Shailen D., Roinard Hélène, Bignalet-Cazalet François, 865 Callahan Philip, Willis Joshua K., Picot Nicolas, Shirtliffe Glenn, Guinle Thierry. “Global Validation of the Version F Geophysical Data Records from the TOPEX/POSEIDON Mission.” 2025.

Forster, L., Desjonquères, J.-D., Talpe, M., Desai, S.D., Roinard, H., Bignalet-Cazalet, F., Callahan, P., Willis, J.K., Picot, N., Shirtliffe, G., Guinle, T.,. “Global Validation of the Version F Geophysical Data Records from the TOPEX/POSEIDON Mission.” *in preparation*, 2025.

870 Gaspar, P., Ogor, F. “Estimation and analysis of the sea state bias of the ERS-1 altimeter.” Technical Report of task B1-B2 of IFREMER Contract, 1994.

Guérou, A., Meyssignac, B., Prandi, P., Ablain, M., Ribes, A., Bignalet-Cazalet, F. “Current observed global mean sea level rise and acceleration estimated from satellite altimetry and the associated measurement uncertainty.” *ocean science* (<https://doi.org/10.5194/os-19-431-2023>), 2023.

875 Guibbaud, M., Ollivier, A., and Ablain, M. “A new approach for dual-frequency ionospheric correction filtering.” ENVISAT Altimetry Quality Working Group (QWG), 2015.

Henry, O., Ablain, M., Meyssignac, B., Cazenave, A., Masters, D., Nerem, S., Leuliette, E., Garric, G. “Investigating and reducing differences between the satellite altimetry-based global mean sea level time series provided by different processing group.” *Journal of Geodesy*, 2013.

880 Hersbach, H., Bell, B., Berrisford, P., Biavati, G., Horányi, A., Muñoz Sabater, J., Nicolas, J., Peubey, C., Radu, R., Rozum, I., Schepers, D., Simmons, A., Soci, C., Dee, D., Thépaut, J-N. “ERA5 hourly data on single levels from 1940 to



present.” <https://doi.org/10.24381/cds.adbb2d47>, <https://cds.climate.copernicus.eu/datasets/reanalysis-era5-single-levels?tab=overview>, 2023.

Heslop, E. E., Sánchez-Román, A., Pascual, A., Rodríguez, D., Reeve, K. A., Faugère, Y., Raynal, M. “Sentinel-3A Views
885 Ocean Variability More Accurately at Finer Resolution.” *Geophysical Research letters*
(<https://doi.org/10.1002/2017GL076244>), 2017.

Ijima, B. A., Harris, I. L., Ho, C. M., Lindqwistle, U. J., Mannucci, A. J., Pi, X., Reyes, M. J., Sparks, L. C., and Wilson, B.
D. “Automated daily process for global ionospheric total electron content maps and satellite ocean altimeter
ionospheric calibration based on Global Positioning System data.” *Journal of Atmospheric and Solar-Terrestrial
890 Physics*, 1999: 1205–1218.

Jettou, G., Rousseau, M., Piras, F., Simeon, M., Tran, N. “SARAL’s Full Mission Reprocessing: Improvement with the
GDR-F Standard.” *Remote Sensing* 15, no. DOI:10.3390/rs15102604 (May 2023).

Kocha, C., Pageot, Y., Rubin, C., Lievin, M., Pujol, M.I., Philipps, S., Prandi, P., Labroue, S., Denis, I., Dibarboure, G.,
Nogueira Loddo, C. “30 years of sea level anomaly reprocessed to improve climate and mesoscale satellite data
895 record.” *OSTST*. Puerto Rico, 2023.

Labroue, S., Ablain, M., Dorandeu, J., Ollivier, A., Phillips, S., Raynal, M., Roinard, H., Picot, N. “Lessons learned from 25
years of cross calibration of the altimetry missions over ocea.” *25 years of progress in radar altimetry symposium.*
Azores, Portugal, 2018.

Laloue, A., Schaeffer, P., Pujol, M-I., Veillard, P., Andersen, O., Sandwell, D., Delepoule, A., Dibarboure, G., Faugère, Y.
900 “Merging Recent Mean Sea Surface Into a 2023 Hybrid Model (From Scripps, DTU, CLS, and CNES).” Fevrier
2025.

Le Traon, P.-Y., Ogor, F. “ERS-1/2 orbit improvement using TOPEX/POSEIDON: The 2 cm challenge.” *JOURNAL OF
GEOPHYSICAL RESEARCH*, 103, 8045-8057 (1998).

Lievin, M., Kocha, C., Courcol, B., Philipps, S., Denis, I., Guinle, T., Nogueira Loddo, C., Dibarboure, G., Picot, N.,
905 Bignalet Cazalet, F. “Reprocessing of Sea Level L2P products for 28 years of altimetry.” *OSTST*. 2020.

Lucas, B. *S3 Altimetry Reprocessing Release Note – BC005*. [https://user.eumetsat.int/s3/eup-strapi-
media/S3_Altimetry_Reprocessing_Release_Note_BC_005_v1_52bc1939bb.pdf](https://user.eumetsat.int/s3/eup-strapi-media/S3_Altimetry_Reprocessing_Release_Note_BC_005_v1_52bc1939bb.pdf), 2023.

Lyard, F. H., Carrere, L., Fouchet, E., Cancet, M., Greenberg, D., Dibarboure, G., Picot, N., “FES2022 a step towards a
SWOT-compliant tidal correction.” *Ocean Sciences*, 2024.

910 Lyard, F.H., Damien, J.A., Cancet, M., Carrere, L., Picot, N. “FES2014 global ocean tide atlas: design and performance.”
Ocean Science 17(3), 615-649, <https://doi.org/10.5194/os-17-615-2021> (2021).

Mertz, F., Mercier, F., Labroue, S., Tran, N., and Dorandeu, J. “ERS-2 OPR data quality assessment long-term monitoring –
Particular investigation.” Technical Report, 2005.



Nencioli, F., Roinard, H., Bignalet-Cazalet, F., Dibarboure, G., and Picot, N. "Advantages and drawbacks of the filtered
915 solution for dual-frequency ionospheric correction from altimetry." *OSTST Meeting*. 2022.

Pascual, A., Lana, A., Troupin, C., Ruiz, S., Faugere, Y., Escudier, R., Tindoré, J. "Assessing SARAL/AltiKa data in the
coastal zone : Comparisons with HF Radar Observations." *Marine Geodesy* 38, 260-276,
https://doi.org/10.1080/01490419.2015.1019656 (2015).

Pujol, M.I. "The 2021 Hybrid MSS product was funded by CNES, produced by CLS in collaboration with Scripps and DTU
920 and made freely available by AVISO". CLS, 2021. 2021 Hybrid Mean Sea Surface (Version 2021) [Data set].
CNES." https://doi.org/10.24400/527896/A01-2021.0, 2021.

Pujol, M-I, Ballarotta, M., Taburet, G., Delepoule, A., Dupuy, S., Kocha, C., Jenn-Alet, M., Dagneaux, Q., Dibarboure, G.,
Faugère, Y.. "DUACS DT-2024: the new reprocessing of the sea level anomaly Level-3&4 altimeter products." "30
Years of progress in radar altimetry" symposium. Montpellier, 2024.

925 Quet, V., Octau, F., Mangilli, A., Prandi, P., Meyssignac, B., Ablain, M., Dibarboure, G. "Estimation of the Topex A /
Topex B bias, A multi methods approach." *OSTST. Puerto Rico*:
https://ostst.aviso.altimetry.fr/fileadmin/user_upload/OSTST2023/Presentations/CVL2023-
Estimation_of_the_Topex_A_B_bias_and_associated_uncertainty_-_A_mutli_methods_approach.pdf, 2023.

Ray, R.D., Schindelegger, M. "Trends in the M2 ocean tide observed by satellite altimetry in the presence of systematic
930 errors." *Journal of Geodesy* 99, no. 11, https://doi.org/10.1007/s00190-025-01935-9 (2025).

Roinard, H., Bignalet-Cazalet, F., Picot N.,. *Jason-2 validation and cross calibration activities (End of mission 2019).*
Validation report, https://www.aviso.altimetry.fr/fileadmin/documents/calval/validation_report/J2/SALP-RP-MA-
EA-23540-CLS_EndOfLife_J2_CalVal_2019_v1-2.pdf, Ramonville Saint-Agne: AVISO, 2022.

Sallée, J.-B., Morrison, A.K., Naughten, K., Thompson, A.F. "Outhern Ocean Circulation, Global Drivers and Ongoing
935 Changes." In *Antarctica and Earth System*, 22. https://doi.org/10.4324/9781003406471, 2025.

Salvatore D., Maraldi C., Cadier E., Rieu P., Aublanc J., Guerou A., Boy F., Moreau T., Picot N., Scharroo R. "Sentinel-6
MF Poseidon-4 radar altimeter: Main scientific results from S6PP LRM and UF-SAR chains in the first year of the
mission." *Advances in Space Research* 73, 1, 337-375, doi:10.1016/j.asr.2023.07.030. (2024).

Sandwell, D.T. "The SIO MSS Sandwell, D. T. (2024). Adding Mean Sea Surface (MSS) as an Altimetry Product." UC San
940 Diego: Scripps Institution of Oceanography., 2024.

Scagliola, M., Recchia, L., Maestri, L., Giudici, D. "Evaluating the impact of range walk compensation in delay/doppler
processing over open ocean." *Adv. Space Res* 68,937-946,https://doi.org/10.1016/j.asr.2019.11.032, no. 2 (2021).

Schaeffer P., Pujol M-I. , Veillard P. , Faugere Y., Dagneau Q. , Sandwell D. , Yu Y. , Harper H.,Andersen, A. Abulaitijiang,
S. Zhang, S-K. Rose,: G. Dibarboure, N. Picot. "The 2023 Hybrid Mean Sea Surface." *SWOT-ST.*
945 //https://doi.org/10.24400/527896/a01-2024.002, 09 2023.



Schaeffer, P., Pujol, M.-I., Veillard, P., Faugere, Y., Dagneaux, Q., Dibarboure, G., Picot, N. "The CNES CLS 2022 Mean Sea Surface: Short Wavelength Improvements from CryoSat-2 and SARAL/AltiKa High-Sampled Altimeter Data. *Remote Sensing*, 15(11), 2910." <https://doi.org/10.3390/rs15112910>, 2023.

Scharroo, R., Smith, W.H.F. "A global positioning system-based climatology for the total electron content in the ionosphere." *Journal of Geophysical Research - Space Physics* 115 (2010).

950 Stammer, D., Cazenave, A., *Satellite Altimetry over Oceans and Land Surfaces*. CRC Press, 2018.

Taburet, G., Sanchez-Roman, A., Ballarotta, M., Pujol, M-I., Legeais, J-F., Faugere, Y., Dibarboure, G. "DUACS DT2018: 25 years of reprocessed." *Ocean Science* 15,1207–1224, <https://doi.org/10.5194/os-15-1207-2019> (2019).

955 Thibaut, P., Piras, F., Roinard, H., Guerou, A., Boy, F., Maraldi, C., Bignalet-Cazalet, F., Dibarboure, G., Picot, N. "Benefits of the "adaptive retracking solution" for the jason-3 gdr-f reprocessing campaign." *International Geoscience and Remote Sensing Symposium IGARSS*. Brussels: IEEE, 2021.

Tourain, C., Piras, F., Ollivier, A., Hauser, D., Poisson, J.C., Boy, F., Thibaut, P., Hermozo, L., Tison, C. "Benefits of the Adaptive Algorithm for Retracking Altimeter Nadir Echoes: Results From Simulations and CFOSAT/SWIM Observations." *Transactions on Geoscience and Remote Sensing* (IEEE) 59, 9927-9940, <https://doi.org/10.1109/TGRS.2021.3064236>, no. 12 (2021).

960 Tran N. "Envisat ESL Phase-F: Tuning activities for Envisat reprocessing baseline v3.0 (Wind, SSB, Rain and Ice)." 2017.

Tran, N. "S3A SSB Solutions. Presented at ESL CM#8 MPC-S3." 2021.

Tran, N. "ESL Cryosat-2: Tuning activities(wind speed and SSB)". 2018.

Tran, N., "Annual Report of SALP Activities : SSB Activity." 2019.

965 Tran, N. "SSB Activity." Annual Rapport of activity SALP, 2015.

Tran, N., Labroue, S., Philipps, S., Bronner, E., Picot, N. "Overview and Update of the Sea State Bias Corrections for the Jason-2, Jason-1 and TOPEX Missions." *Marine Geodesy*, no. 33 (2010): 348–362.

Tran, N., Philipps, S., Poisson, J.-C., Urien, S., Bronner, E., and Picot, N. "Impact of GDR_D standards on SSB corrections." *OSTST Meeting*. Venise, 2012.

970 Ubelmann, C., Dibarboure, G., Gaultier, L., Ponte, A., Arduin, F., Ballarotta, M., Faugère, Y. "Reconstructing Ocean Surface Current Combining Altimetry and Future Spaceborne Doppler Data." *Journal of Geophysical Research Ocean* 126, e2020JC016560, <https://doi.org/10.1029/2020JC016560> (2021).

Van Gysen, H., Coleman, R., Hirsch, B. "Local crossover analysis of exactly repeating satellite altimeter data." *Journal of geodesy*, 1997: 31-43.

975 Vergara, O., Morrow, R., Pujol, M.I., Dibarboure, G., Ubelmann, C. "Global submesoscale diagnosis using along-track satellite altimetry." *Ocean Science* 19, 363-379, <https://doi.org/10.5194/os-19-363-2023> (2023).

Zaron, E. D. "Baroclinic Tidal Sea Level from Exact-Repeat Mission Altimetry." *J. Phys. Oceanogr.* 49 (2019): 193–210.



980 Zawadzki, L., Ablain M. "Accuracy of the mean sea level continuous record with future altimetric missions: Jason-3 vs. Sentinel-3a." *ocean science* (https://os.copernicus.org/articles/12/9/2016/os-12-9-2016.pdf, https://doi.org/10.5194/os-12-9-2016), 2016.

Zhang, S., Li, J., Jin, T., Che, D. "HY-2A Altimeter Data Initial Assessment and Corresponding Two-Pass Waveform Retracker." *Remote Sensing* 10 (4), 507. doi:10.3390/rs10040507 (2018).

The DT-2024 Level-2P dataset is available to users for all the altimeter missions on AVISO+ (https://doi.org/10.24400/527896/a01-2025.004). The Level-3 and Level-4 counterparts are available on the Copernicus Marine Service catalogue (https://marine.copernicus.eu) and C3S (https://cds.climate.copernicus.eu):

- Level-2P Global Ocean Multi-Year product: <https://doi.org/10.24400/527896/a01-2025.004>
- Level-3 Global Ocean Multi-Year product: <https://doi.org/10.48670/moi-00146>
- Level-3 European Seas Multi-Year product: <https://doi.org/10.48670/moi-00139>
- Level-4 Global Ocean Multi-Year product: <https://doi.org/10.48670/moi-00148>
- Level-4 European Seas Multi-Year product: <https://doi.org/10.48670/moi-00141>
- Level-4 Climate-focused product: <https://doi.org/10.48670/moi-00145> or [10.24381/cds.4c328c78](https://doi.org/10.24381/cds.4c328c78)